

Survey paper

Medical artificial intelligence for early detection of lung cancer: A survey



Guohui Cai^a, Ying Cai^a,*, Zeyu Zhang^b, Yuanzhouhan Cao^c, Lin Wu^d, Daji Ergu^a, Zhibin Liao^e, Yang Zhao^f

^a College of Computer Science and Artificial Intelligence, Southwest Minzu University, Chengdu, 610225, China

^b The Australian National University, Canberra, ACT 2601, Australia

^c School of Computer Science and Technology, Beijing Jiaotong University, Beijing, China

^d Hunan University of Technology, Zhuzhou, 410072, China

^e University of Adelaide, Adelaide, South Australia 5005, Australia

^f La Trobe University, Melbourne, Victoria 3086, Australia

ARTICLE INFO

Dataset link: <https://github.com/CaiGuoHui123/Awesome-Lung-Cancer-Detection>

Keywords:

Lung cancer detection
Deep learning
Artificial intelligence
Pulmonary nodule detection
Computer-aided diagnosis
Pulmonary nodule segmentation and classification

ABSTRACT

Lung cancer remains one of the leading causes of morbidity and mortality worldwide, making early diagnosis critical for improving therapeutic outcomes and patient prognosis. Computer-aided diagnosis systems, which analyze computed tomography images, have proven effective in detecting and classifying pulmonary nodules, significantly enhancing the detection rate of early-stage lung cancer. Although traditional machine learning algorithms have been valuable, they exhibit limitations in handling complex sample data. The recent emergence of deep learning has revolutionized medical image analysis, driving substantial advancements in this field. This review focuses on recent progress in deep learning for pulmonary nodule detection, segmentation, and classification. Traditional machine learning methods, such as support vector machines and k-nearest neighbors, have shown limitations, paving the way for advanced approaches like Convolutional Neural Networks, Recurrent Neural Networks, and Generative Adversarial Networks. The integration of ensemble models and novel techniques is also discussed, emphasizing the latest developments in lung cancer diagnosis. Deep learning algorithms, combined with various analytical techniques, have markedly improved the accuracy and efficiency of pulmonary nodule analysis, surpassing traditional methods, particularly in nodule classification. Although challenges remain, continuous technological advancements are expected to further strengthen the role of deep learning in medical diagnostics, especially for early lung cancer detection and diagnosis. A comprehensive list of lung cancer detection models reviewed in this work is available at <https://github.com/CaiGuoHui123/Awesome-Lung-Cancer-Detection>.

1. Introduction

Lung cancer is one of the leading causes of both incidence and mortality worldwide. According to the latest assessment by the International Agency for Research on Cancer (IARC) of the World Health Organization (WHO), in 2022, there were approximately 19.96 million new cancer cases globally, with 2.48 million of them being lung cancer, accounting for 12.4% of all cases, making it the most prevalent cancer worldwide (Fig. 1) (Bray et al., 2024). Due to the subtlety of early-stage lung cancer symptoms, patients often miss the optimal treatment window. Early screening and computed tomography (CT) scans are essential for early diagnosis, as they allow for the detection of lesions before clinical symptoms manifest, significantly increasing the rate of early lung cancer detection. Computer-aided diagnosis (CAD) systems are designed to assist in medical image analysis by automating the

detection of abnormalities, such as those in CT scans (Jin et al., 2023). These systems improve diagnostic accuracy and reduce the workload of radiologists. In lung cancer detection, CAD systems are particularly effective in identifying and assessing pulmonary nodules. With advances in deep learning and artificial intelligence, these systems have become increasingly accurate, fast, and reliable, supporting early lung cancer diagnosis.

Pulmonary nodules are defined as round or irregular lesions with a diameter of less than 30 mm, typically appearing on CT images as high-density areas with either well-defined or blurred margins. Nodules can be categorized into solid, subsolid, and ground-glass types based on their density and morphology. Among these, solid nodules generally pose a lower risk of malignancy, whereas subsolid and ground-glass nodules, particularly those that are large and irregular, are associated with a higher risk. Consequently, accurate identification and

* Corresponding author.

E-mail address: caying34@yeah.net (Y. Cai).

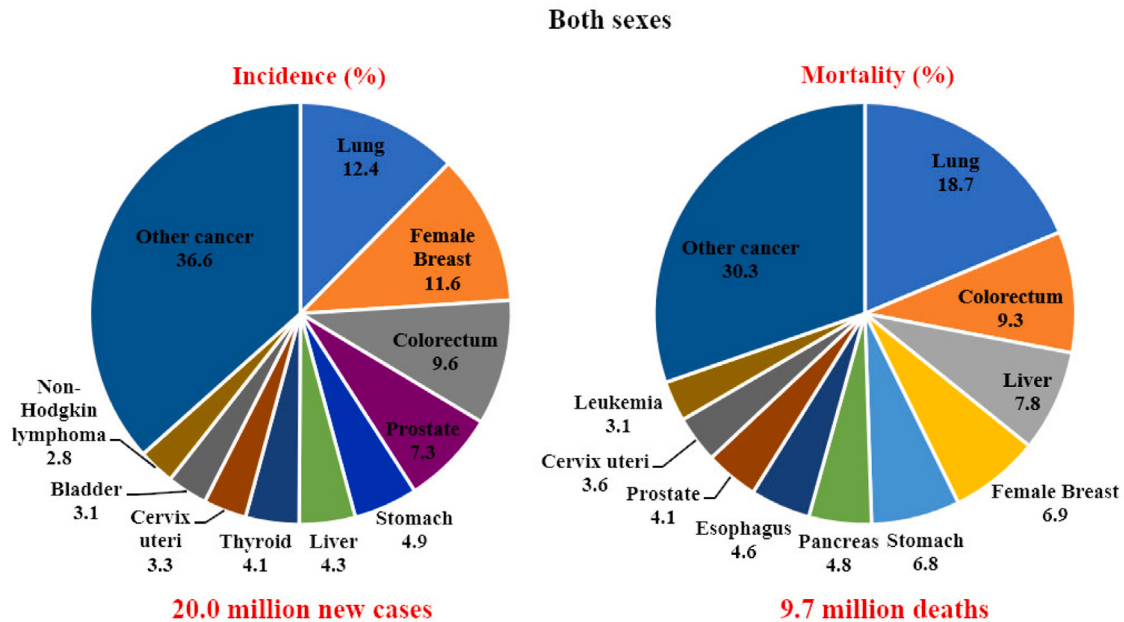


Fig. 1. Pie chart showing the distribution of cases and deaths in 2022 for the top five cancers and an aggregated “Others” category (all remaining cancer types). The area of each slice reflects its proportion of the total number of cases or deaths (Bray et al., 2024).

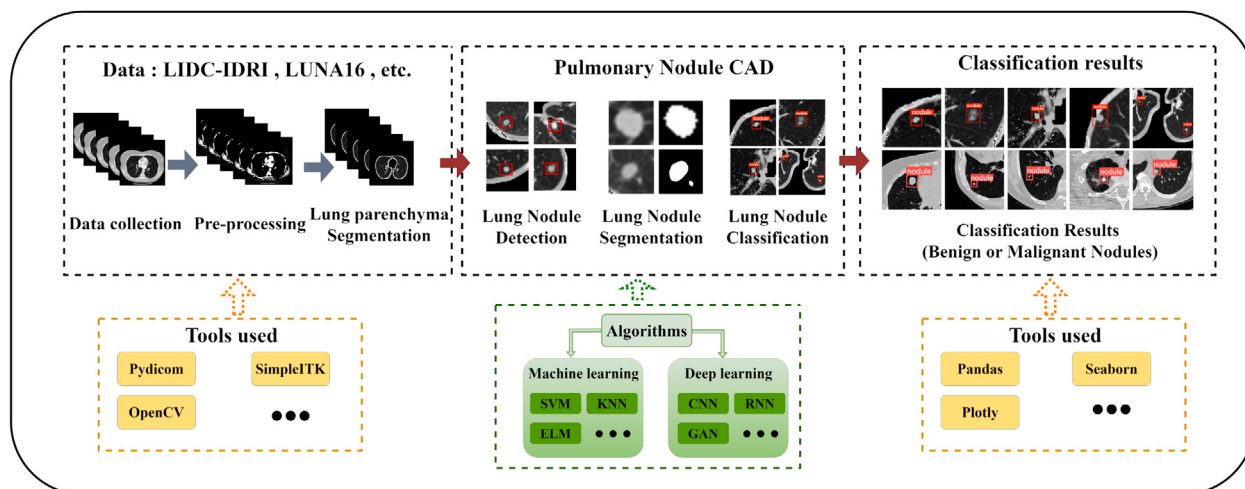


Fig. 2. Framework of this study and the basic steps of the pulmonary nodule CAD system.

classification are critical for clinical diagnosis (Zhang et al., 2024a; Hiwase et al., 2024). The application of computer-aided detection (CAD) technology in lung cancer diagnosis began in the 1980s, initially focusing on assisting in the detection of abnormalities on chest X-rays. It later expanded to high-resolution CT image analysis, evolving from simple image processing to sophisticated deep learning models that significantly enhance both sensitivity and specificity. Today, CAD systems can autonomously detect and evaluate pulmonary nodules, provide follow-up recommendations, and assist in decision-making, substantially improving the accuracy and efficiency of early lung cancer screening.

Compared to traditional machine learning (ML) methods, deep learning, particularly convolutional neural networks (CNNs), has demonstrated superior performance in pulmonary nodule CAD systems (Krizhevsky et al., 2012). Traditional ML relies on manually extracted features, which are limited by the quality of the features, whereas deep learning can automatically learn complex image features, significantly improving detection accuracy and robustness. This advantage is especially apparent in handling high-dimensional and

large-scale data, where deep learning excels at capturing subtle changes in pulmonary nodules, thereby enhancing diagnostic efficiency. The workflow of a pulmonary nodule CAD system includes CT image preprocessing, automatic segmentation of nodule regions, feature extraction, and classification analysis, ultimately generating diagnostic reports that assist clinicians in decision-making. The system aims to improve detection accuracy and efficiency, contributing to early lung cancer diagnosis.

Recent reviews have summarized the application of AI in early lung cancer detection. The study by Kaulgud and Patil (2023) primarily focuses on CT image detection methods and compares the performance of various techniques in pulmonary nodule detection. Similarly, Kalke-seetharaman and George (2024) review studies based on X-ray and CT images, highlighting the advantages of deep learning in CT image-based pulmonary nodule detection. However, these reviews lack an in-depth exploration of the differences between traditional machine learning and deep learning algorithms, particularly in terms of data sources and nodule segmentation methods, which is a significant oversight (Kaulgud

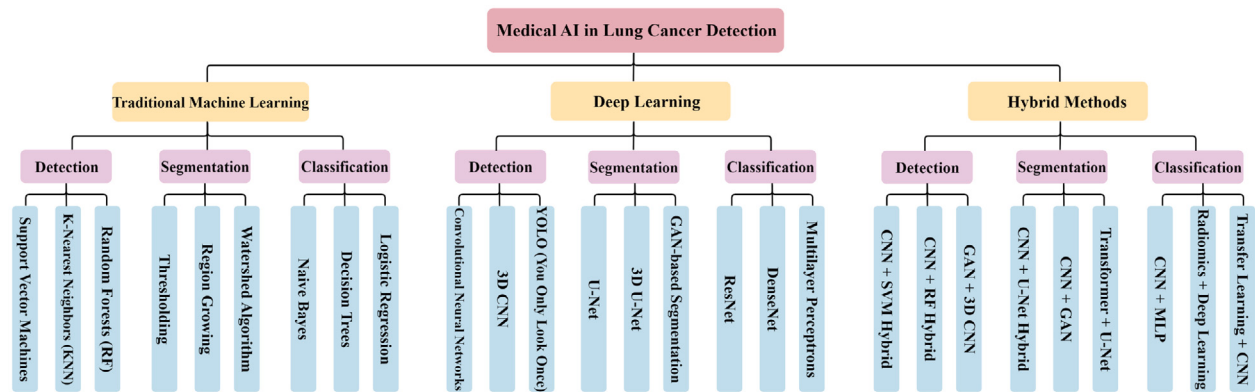


Fig. 3. This tree diagram illustrates the overall development of medical AI technologies in the early detection of lung cancer. The diagram provides an overview of key advancements and techniques in the field, structured into three main sections: Traditional Machine Learning, Deep Learning, and Hybrid Methods. Each section is further divided into three core tasks—Detection, Segmentation, and Classification—highlighting key techniques used in each. Traditional methods like Support Vector Machines (SVM), Thresholding, and Decision Trees have been foundational, while deep learning methods such as CNN, U-Net, and ResNet have significantly advanced the field, especially after the rise of deep learning in 2012. Hybrid methods, combining models from both machine learning and deep learning, have become prominent since 2018, offering enhanced accuracy and robustness.

and Patil, 2023). They also provide insufficient descriptions of specific algorithms and model characteristics, lacking a unified review framework (Kalkseetharaman and George, 2024).

To address these gaps, this review discusses the application of AI technologies in early lung cancer detection and diagnosis, aiming to leverage AI for the rapid detection (Zhao et al., 2024), segmentation (Ge et al., 2024), and classification of pulmonary nodules. The research framework is illustrated in Fig. 2, and the overall development of medical AI technologies in lung cancer detection is shown in Fig. 3.

The main contributions of this review are as follows:

- A comprehensive analysis of diverse data sources and a systematic literature retrieval and screening process, identifying key studies and trends in lung cancer detection.
- A discussion of the structure, performance, and applicable scenarios of traditional machine learning and deep learning algorithms for lung cancer analysis.
- An in-depth comparison of lung cancer detection, segmentation, and classification tasks across 131 reviewed studies, highlighting their respective strengths, limitations, and future research directions.
- Practical insights into designing high-performance lung cancer analysis workflows, optimizing computational complexity, and enhancing model interpretability, providing valuable guidance for researchers and radiologists.

2. Medical AI for lung cancer detection

In recent years, the rapid advancement of artificial intelligence has brought unprecedented transformations across various industries, particularly in the field of lung cancer detection and diagnosis. Traditional methods for detecting pulmonary nodules often rely on the expertise of radiologists, are time-consuming, and are influenced by subjective factors, which can compromise the accuracy of diagnostic results. However, with the progress of AI technology, the healthcare sector has embraced new possibilities. AI enables machines and computer systems to emulate human intelligence, encompassing capabilities such as language comprehension, natural language processing, decision-making, and visual perception, as discussed by Bawack et al. (2021). The robust learning capabilities and high precision of AI have led to its increasing application in lung cancer detection, particularly in the analysis of medical images. Through deep learning algorithms, AI can automatically identify and analyze pulmonary nodules, significantly enhancing the accuracy of early diagnosis and assisting physicians in making timely and effective decisions, ultimately improving patient survival rates.

2.1. Statistical learning based

Machine learning is a methodology for implementing artificial intelligence that utilizes statistical learning algorithms to enable computer systems to learn from experience and improve performance. In this process, manually designed feature engineering is crucial for transforming data into a format suitable for shallow models. As illustrated in Fig. 4, statistical learning-based algorithms include Support Vector Machines (SVM) (Cortes and Vapnik, 1995), K-Nearest Neighbors (KNN) (Cover and Hart, 1967), Extreme Learning Machines (ELM) (Huang et al., 2006), Decision Trees (DT), Random Forests (RF), and Naive Bayes (NB). These methods have been widely applied in medical imaging analysis, particularly in the detection of pulmonary nodules, significantly improving diagnostic accuracy and assisting physicians in identifying potential malignant lesions in a timely manner.

Despite their commendable performance in this field, statistical learning-based methods have certain limitations. They often rely on manual feature design and selection, which can be time-consuming and heavily influenced by domain knowledge; improper feature selection may adversely affect model performance. Additionally, these algorithms face challenges in effectively handling nonlinearity, high-dimensional data, and complex data relationships, particularly when dealing with unstructured data such as lung imaging, where capturing latent patterns and structures proves difficult. However, the advent of deep learning methods offers effective solutions to these challenges. Deep learning has significant advantages over statistical learning-based methods, with the main differences shown in Fig. 5a. Deep learning models can autonomously learn feature representations from raw data, eliminating the need for tedious manual feature engineering. The operation process of a deep neural network is illustrated in Fig. 5b.

2.2. Convolutional Neural Network (CNN)

Convolutional Neural Networks (CNNs) originated in the 1980s with the development of LeNet by Yann LeCun's team for handwritten digit recognition (LeCun et al., 1998). The rapid advancements in computational power and large-scale datasets facilitated the widespread adoption of CNNs in the early 21st century, culminating in the success of AlexNet in the 2012 ImageNet competition, which marked a significant milestone (Krizhevsky et al., 2012). Subsequent architectures like DenseNet and ResNet further improved classification accuracy (He et al., 2016), significantly advancing both computer vision and medical image analysis. Today, CNNs have become the cornerstone of modern medical image analysis, particularly in the detection (Zhang

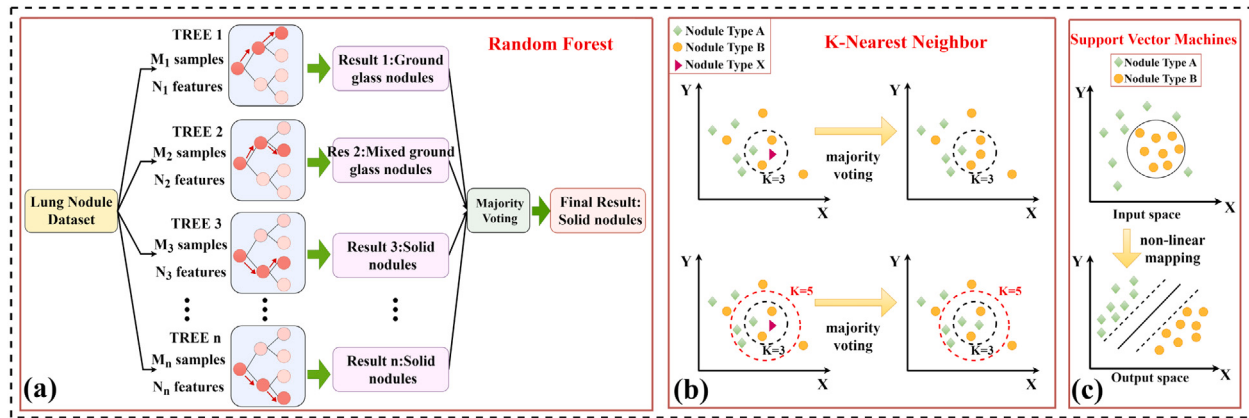


Fig. 4. Algorithm structure schematic. (a) Random Forest (RF) incorporates multiple decision trees to evaluate different aspects of the pulmonary nodule dataset, with a majority vote determining the final category of each nodule. (b) K-Nearest Neighbor (KNN) classifies nodules by analyzing the closest training examples in the feature space, employing a specific number of neighbors (e.g., $K = 3$) for voting. (c) Support Vector Machine (SVM) constructs a hyperplane to distinctly separate different types of nodules, optimizing classification based on their features. Each method effectively leverages feature information along the X and Y axes to distinguish between nodule types.

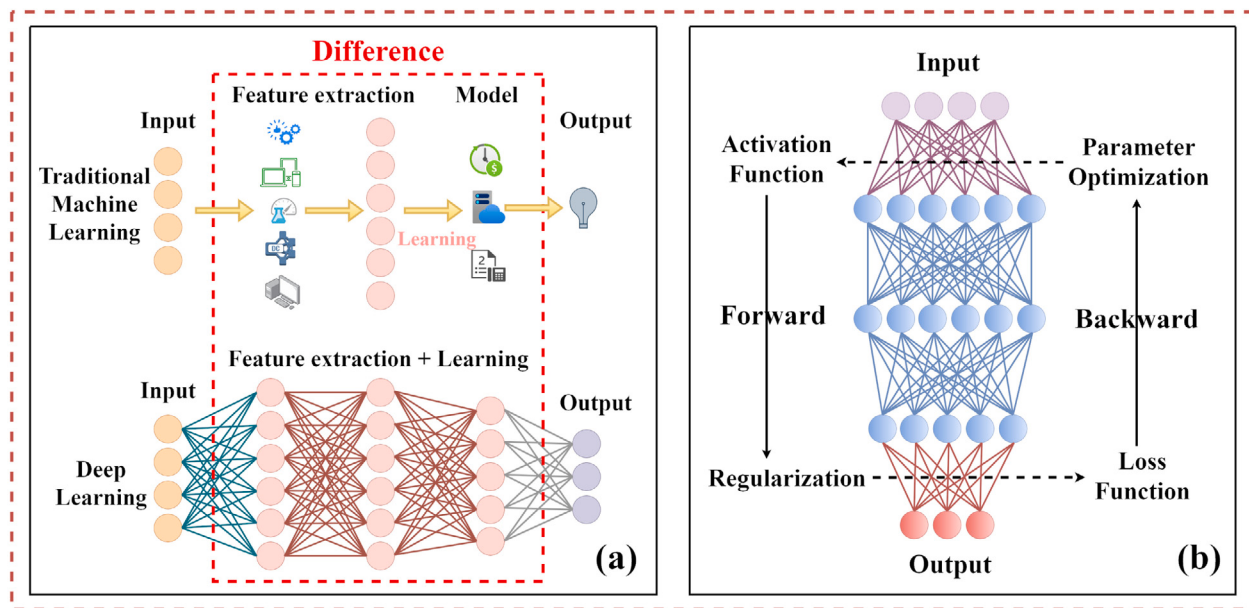


Fig. 5. (a) Main difference between statistical learning-based and deep learning. Statistical learning-based methods rely on manually extracted features and employ simpler algorithms that often require human intervention for optimal performance. In contrast, deep learning automates the feature extraction process, utilizing complex neural network architectures that learn directly from raw data. This capability enables deep learning to handle more complex data structures and patterns, improving accuracy and efficiency in tasks such as medical image analysis. (b) The deep neural network operation process.

et al., 2024g), segmentation (Wu et al., 2023b; Zhang et al., 2024f, 2023), and classification of pulmonary nodules in CT scans. Designed to automatically and adaptively learn spatial hierarchies of features from input images through multiple layers of convolutional filters, CNNs capture intricate patterns and textures inherent in medical imaging data, making them exceptionally well-suited for identifying subtle abnormalities such as pulmonary nodules. Fundamental architectures such as LeNet, AlexNet, VGG, ResNet, and, more recently, specialized models like U-Net and DenseNet, have been extensively employed and further refined to enhance the precision and efficiency of lung cancer detection systems. The basic structure of a CNN is shown in Fig. 6b.

In addition to CNNs, Multilayer Perceptrons (MLPs) have historically served as foundational models in deep learning, consisting of an input layer, multiple hidden layers, and an output layer, as shown in Fig. 6a. While MLPs excel at capturing higher-order abstract features within data, their application to complex, high-dimensional tasks like pulmonary nodule classification often leads to increased computational costs and challenges such as overfitting. To overcome these limitations,

researchers have integrated MLPs with CNN architectures, leveraging the strengths of both models. For instance, Zhu et al. (2018) enhanced nodule detection by combining convolutional layers with MLP components in CM-Net, effectively capturing local dependencies in CT images while maintaining computational efficiency.

When comparing various CNN-based approaches for pulmonary nodule analysis, several studies demonstrate significant advancements in both accuracy and computational efficiency. For instance, Kadhim et al. (2022) developed a high-efficiency CAD system using CNNs and stacked autoencoders, achieving an accuracy of 99.0% on the LIDC-IDRI dataset. Similarly, Bhatt et al. (2022) employed the YOLOv4 model, which attained 95% precision and 81% sensitivity, showcasing real-time detection capabilities. de Mesquita et al. (2022) introduced a Boolean equation-based method integrated with CNNs, achieving 92.75% sensitivity with 8 false positives per scan. Additionally, Suzuki et al. (2022) enhanced a 3D U-Net model, reaching a CPM of 94.7% on the LIDC-IDRI dataset and 83.3% on a Japanese dataset, demonstrating robust cross-dataset performance. These studies highlight the

Table 1
Typical applications of CNN models in pulmonary nodule detection, segmentation, and classification on CT images.

Task Type	Authors	Year	2D/3D	Technique/ network type	Validation/ test method	Nodules types	Main method	Model performance
Detection	Kadhim et al. (2022)	2022	2D and 3D	CNN; SAE	Accuracy, Sensitivity	Multiple appearances and shapes (size <10 mm)	Pulmonary nodule detection and diagnosis with CAD	Performance varies based on dataset used, comparison of CAD methods
	Bhatt et al. (2022)	2022	2D	YOLOv4	Sensitivity	Various nodule types	YOLOv4 model	Sensitivity with FP/scan: 81%
	de Mesquita et al. (2022)	2022	3D	CNN	10-fold cross-validation	Nodules larger than 3 mm	Nodule detection using 16 filters and Boolean logic	Sensitivity: 92.75%, 8 false positives per exam with majority gold standard
	Suzuki et al. (2022)	2022	3D	CNN; 3D U-Net	Sensitivity	Nodules > 5 mm	Automated nodule detection with 3D U-Net	Internal CPM: 94.7%, External CPM: 83.3%
	Karrar et al. (2023)	2022	2D and 3D	SVM, DCNN	10-fold cross-validation	Solitary, juxtapleural	CADx: segmentation, SVM, DCNN	SVM: 91.4%, DCNN: 95%
	Bhaskar et al. (2023)	2023	3D	U-net, CNN	80:20 train-test split	Cancerous or non-cancerous	U-net for segmentation, CNN for classification	Sensitivity: 0.75 (before), 0.65 (after classification)
	Jian et al. (2024)	2024	3D	Dual-branch, 3D CNN	5-fold cross-validation	Lung parenchyma and chest wall nodules	Multi-task dual-branch 3D CNN, attention fusion	Sensitivity: 91.33%, 0.125 to 8 FPs/scan
Segmentation	Zhao et al. (2023)	2023	3D	3DCNN	10-fold cross-validation	Types, shapes, sizes: 3–30 mm	Adaptive 3D CNN	Sensitivity: 0.947, FP/s: 0.14
	Ahmadyar et al. (2024)	2024	2D and 3D	YOLOv5s, 3DCNN	Evaluated on LUNA16	Pulmonary nodules	Hierarchical YOLOv5s, 3DCNN	Sensitivity: 97.8%, confidence: 0.3
	Ma et al. (2024a)	2024	3D	Transformer, CNN	10-fold cross-validation	Benign and malignant	TICNet, Transformer, attention, multi-scale fusion	Sensitivity: 93%, <11 FP/scan, CPM: 90.73%
	Sweetline et al. (2024)	2024	2D	Multi-crop CNN	Sensitivity	Various nodule types	Multi-crop CNN, boundary refinement, seg	DSC:LUNA16:0.978, LIDC:0.982, Sensitivity: LUNA16:97.6%, LIDC:98%
	Zhang et al. (2024d)	2024	2D	DS-MSFF-Net	Sensitivity	Benign and malignant	Dual-path: semantic feature extraction	LIDC-IDRI: 85.39%, LiTS2017 liver: 95.79%, LiTS2017 tumor: 91.75%
	Suji et al. (2024)	2024	2D	UNet, FPN, PSPNet	Sensitivity	Various nodule types	Pretrained encoders: ResNet	DSC: IoU (UNet-efficientnet-b3): 0.5922
	Asiya and Sugitha (2024)	2024	2D	Custom-VGG16	Sensitivity	Benign and malignant	Custom-VGG16: preprocessing	Precision: 90.87%
Classification	Tang et al. (2023b)	2023	2D	SM-RNet	Sensitivity	Benign and malignant	SM-RNet: Weighted-fusion	Precision: FUSCC: 89.774%, LUNA16: 85.047%
	Cai et al. (2024b)	2024	2D	MDFN	5-fold cross-validation	Various nodule types	MDFN: Self-calibrated edge enhancement	DSC: 89.19%; Sensitivity: 88.89%
	Fu et al. (2021)	2021	3D	MLP; Mr-Mc	5-fold cross-validation	Inflammation, squamous cell carcinoma	Double modal fusion of CT images and LTBs	Mr-Mc Acc: 0.810, MLP Acc: 0.887, Fusion model Acc: 0.906
	Zhan et al. (2023)	2023	3D	3D CNN: SSL	5-fold cross-validation	Solitary Pulmonary Nodules (SPNs)	SSL with USC for supervised training	Supervised: Acc: 0.662, USC (confidence): Acc: 0.702, Sensitivity: 0.707
	Rahouma et al. (2024)	2024	3D	3D CNN + GA	4-fold cross-validation	Benign or Malignant	3D CNN with GA for design	95.98%, Sensitivity: 98.80%, AUC: 0.985, Specificity: 93.40%
	Lin et al. (2024a)	2024	3D	3D CNN	10-fold cross-validation	IA, MIA, AIS, and AAH	AutoGluon-Tabular for classification	Task 1: Acc: 92.8%, Sensitivity: 89.43%, AUC: 96.17%, Task 2.1: Acc: 74.76%
	Drishti and Singh (2024)	2024	2D	CNN - ConvNet	5-fold cross-validation	benign or Malignant	Multi-scale, multi-path for feature extraction	Acc: 90.38%, Sensitivity: 88.70%, AUC: 0.948, Specificity: 92.40%

versatility and robustness of CNN architectures in diverse clinical settings, effectively handling different nodule types and minimizing false positives.

Furthermore, the integration of MLPs within CNN frameworks has led to the development of more sophisticated models that combine feature extraction with complex classification tasks. For example, Fu et al. (2021) introduced a multimodal diagnostic model that integrates 3D lung CT images with serum biomarkers, achieving an average accuracy of 90.6% on the LIDC-CISB dataset by fusing a multi-resolution 3D multi-class deep learning model (Mr-Mc) with an MLP model based on lung tumor biomarkers (LTBs). This integration underscores the potential of hybrid models in enhancing the accuracy and reliability of pulmonary nodule detection and classification.

In summary, CNNs are pivotal to modern computer-aided diagnosis (CAD) systems for lung cancer, offering unmatched capabilities in feature extraction and pattern recognition. Models such as Kadhim et al.'s (2022) CNN with stacked autoencoders, Bhatt et al.'s (2022) YOLOv4, de Mesquita et al.'s (2022) Boolean equation-based CNN, Suzuki et al.'s (2022) enhanced 3D U-Net, and the MLP-integrated approaches by Zhu et al. (2018) and Fu et al. (2021) demonstrate significant strides in improving the accuracy, sensitivity, and specificity of pulmonary nodule detection and classification. These advancements not only facilitate early diagnosis and optimize treatment planning but also support the seamless integration of CNN-based systems into routine

clinical workflows, thereby elevating the standards of lung cancer care. The typical CNN applications in this field in recent years are listed in Table 1.

2.3. Recurrent Neural Network (RNN)

Recurrent Neural Networks (RNNs), introduced by Rumelhart et al. in 1986 (Rumelhart et al., 1986), are designed to handle sequential data by maintaining an internal state that captures information from previous inputs. This makes RNNs particularly effective for tasks involving temporal dependencies, such as language processing and the detection of pulmonary nodules from continuous imaging datasets. Traditional RNNs, however, face challenges like vanishing and exploding gradients, limiting their ability to learn long-term dependencies. To address these issues, architectures such as Long Short-Term Memory (LSTM) networks and Gated Recurrent Units (GRUs) were developed (Hochreiter and Schmidhuber, 1997), employing gating mechanisms to control the flow of information and retain context over longer sequences. In pulmonary nodule detection, these models improve accuracy by learning inter-slice dependencies in CT images. Furthermore, Bidirectional RNNs and attention mechanisms enhance the network's ability to focus on important parts of the sequence, increasing detection precision. With these advancements, RNNs and their variants have become essential

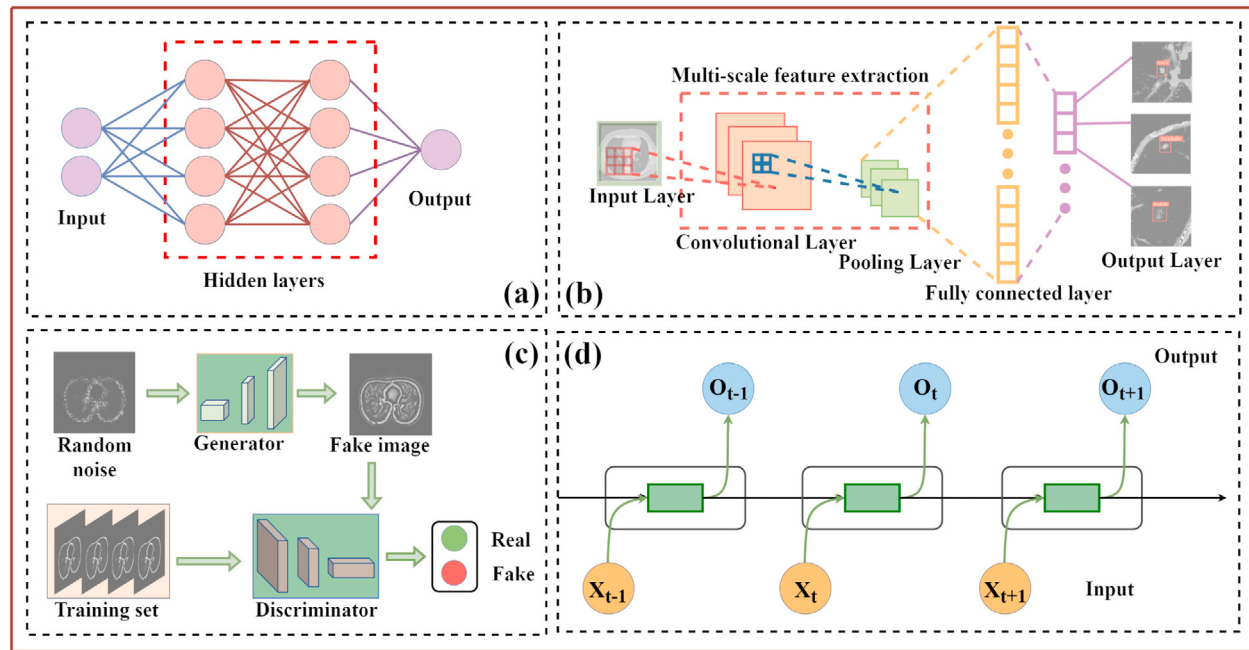


Fig. 6. Various deep learning models and structures: (a) Multilayer Perceptron (MLP) performs complex function approximation, vital for pattern recognition in data structures. (b) Convolutional Neural Network (CNN) excels in automatic feature extraction and analyzing structural details in lung CT scans. (c) Generative Adversarial Network (GAN) synthesizes accurate medical images, mitigating the lack of annotated samples and improving model robustness. (d) Recurrent Neural Network (RNN) analyzes temporal patterns in sequential lung scans, crucial for accurate pulmonary nodule detection.

tools in medical image analysis, particularly in the early detection of lung cancer, as illustrated in Figs. 6d and 7a.

In the analysis of pulmonary nodules, RNNs, with their unique ability to process temporal sequences, are capable of capturing sequential patterns in CT scan data, significantly improving classification tasks. For instance, [Balannolla et al. \(2022\)](#) combined RNNs with convolutional layers for pulmonary nodule classification, achieving a sensitivity of 96.4% using KNN classifiers. Similarly, [Gugulothu and Balaji \(2024\)](#) employed an RNN model integrated with feature selection algorithms for nodule classification, reaching a classification accuracy of 93.6% and a sensitivity of 96.39%. The advantage of RNNs in these medical imaging tasks lies in their ability to handle temporal dependencies within sequential data, thereby effectively improving the robustness and accuracy of classification. However, the complexity and high computational demands of RNNs remain challenges that need optimization, with researchers continuously exploring novel network architectures and optimization strategies to address these issues.

Although significant progress has been made in pulmonary nodule detection using convolutional neural networks (CNNs) in recent years, RNNs, as a deep learning method capable of processing temporal information, continue to show potential in enhancing performance when integrated with other network architectures. For example, some studies have combined RNNs with CNNs to improve nodule detection, offering the dual advantage of handling both spatial and temporal features. Additionally, methods such as the adaptive anchor box Faster R-CNN proposed by [Nguyen et al. \(2023\)](#), which integrates RNNs, and the dual-stage framework developed by [El-Bana et al. \(2020\)](#), where RNN modules enhance classification tasks, have made significant progress in improving detection sensitivity and reducing false positives. These studies illustrate that the application of RNNs in medical imaging extends beyond classification tasks, and when combined with other neural networks, can further enhance the recognition and handling of complex data patterns, thereby advancing the field of pulmonary nodule detection.

2.4. Generative Adversarial Network (GAN)

Generative Adversarial Networks (GANs), introduced by Ian Goodfellow and colleagues in 2014 ([Goodfellow et al., 2014](#)), consist of two neural networks—the generator and the discriminator—that are trained simultaneously through an adversarial process. The basic structure is shown in Fig. 6c. The generator aims to produce realistic data samples, while the discriminator attempts to distinguish between genuine data and those generated by the generator. This competitive dynamic drives the generator to produce increasingly realistic data, enhancing its capacity to model complex data distributions. In medical imaging, GANs have been extensively applied to tasks such as image synthesis, restoration, and super-resolution, significantly improving the accuracy and robustness of pulmonary nodule detection. Variants of GANs, such as Conditional GANs, Generative Adversarial Autoencoders, and CycleGANs, provide specialized solutions for specific challenges. For example, Conditional GANs generate images with specific pathological features, increasing data diversity, while Generative Adversarial Autoencoders produce high-resolution images that assist in the precise identification of nodules. CycleGANs, notably, can improve image quality without the need for paired datasets, which is particularly beneficial in medical scenarios with limited annotated data. By generating high-fidelity synthetic data for data augmentation, GANs help address issues of limited and imbalanced datasets, resulting in enhanced model performance and generalization. Overall, GANs and their variants play a crucial role in enriching diagnostic data and driving advancements in medical image analysis, especially for the early detection of pulmonary nodules.

In the realm of pulmonary nodule analysis, GANs have been employed to tackle challenges related to data scarcity and class imbalance. For instance, [Sengodan et al. \(2023\)](#) applied GANs to generate synthetic CT images of pulmonary nodules, augmenting the training dataset and improving the robustness of detection models. In another study, [Zhu et al. \(2021b\)](#) incorporated GAN-based data augmentation into a dual-branch CNN framework, leading to improved segmentation accuracy

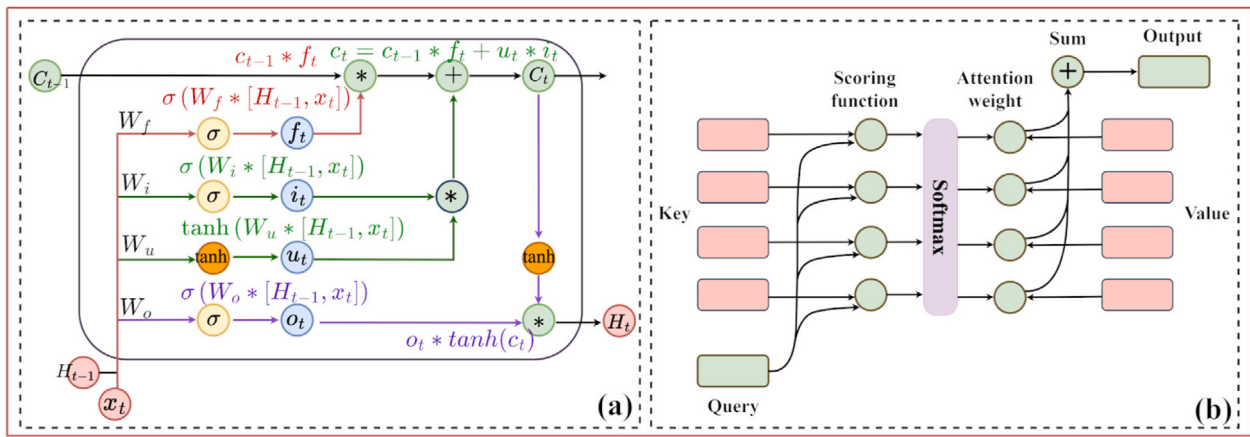


Fig. 7. Various deep learning models and structures: (a) Long Short-Term Memory (LSTM) structure is vital for sequence data analysis in medical applications, utilizing forget, input, and output gates to manage information flow, thereby maintaining essential temporal features critical for accurate diagnostic predictions. This mechanism proves especially effective in analyzing diagnostic time-series data, capturing crucial changes over time. (b) The Attention Mechanism enhances neural network focus on significant features within diagnostic images, facilitating precise detection and categorization of anomalies such as tumors and lesions by adjusting the model's focus to the most informative regions of the image data.

and reduced false positives. Furthermore, Gugulothu and Balaji (2023) introduced a deep learning method that integrates step deviation mean multi-level thresholding (SDMMT) and a novel CSDR-J-WHGAN classifier, achieving impressive classification results with 97.11% detection accuracy on the LIDC-IDRI dataset. Zhu et al. (2021a) further enhanced GAN-based approaches by developing the Functional Realistic GAN (FRGAN) architecture, which employs TreeGAN to generate high-resolution images with accurate pathological features, significantly improving detection sensitivity and accuracy, as demonstrated by its CPM score of 0.915 on the LUNA16 dataset.

Moreover, Tyagi and Talbar (2022) proposed a 3D Conditional GAN (CSE-GAN) for pulmonary nodule segmentation, integrating a U-Net-based generator with parallel compression and excitation modules. This approach effectively reduced overfitting and improved segmentation performance, achieving a Dice coefficient of 80.74% on the LUNA16 dataset. These advanced GAN-based methods not only enhance training datasets with high-quality synthetic images but also improve segmentation and classification accuracy, effectively addressing issues related to data scarcity and class imbalance. On the other hand, we have greatly enriched our discussion of Generative Adversarial Networks (GANs) by detailing not only their applications in data augmentation but also the quantitative metrics used to assess the quality and realism of synthetic medical images. Key evaluation measures now include the Fréchet Inception Distance (FID), which quantifies distributional similarity between generated and real images in the feature space of a pretrained network (lower is better); the Inception Score (IS), which captures both image quality and diversity via entropy-based measures (higher is better); the Structural Similarity Index Measure (SSIM), commonly used in medical imaging to assess perceptual similarity between synthetic and original CT slices; and the Peak Signal-to-Noise Ratio (PSNR), which evaluates reconstruction fidelity. We further introduce the concept of a Visual Turing Test (VTT), wherein expert radiologists attempt to distinguish synthetic from real images as a subjective but clinically pertinent validation. Finally, we reference recent studies—such as Gugulothu et al. (2023)—that employ GANs for both image synthesis and enhancement, demonstrating improvements in downstream classification performance when augmented with high-quality synthetic data.

In summary, GANs provide innovative solutions for pulmonary nodule analysis by generating realistic synthetic data that mitigates the challenges of data scarcity and class imbalance. Studies by Sengodan et al. (2023), Zhu et al. (2021b), Gugulothu and Balaji (2023), Zhu et al. (2021a), and Tyagi and Talbar (2022) demonstrate the effectiveness of GAN-based augmentation in enhancing the performance and robustness

of detection and segmentation models. These findings underscore the growing potential of GANs in clinical applications for pulmonary nodule detection, presenting a promising avenue for improving diagnostic accuracy and reliability. As GAN technology continues to evolve, its remarkable ability to generate high-quality synthetic data has attracted increasing attention, highlighting its critical role in the development of next-generation CAD systems for early lung cancer detection and diagnosis.

2.5. Transformer based methods

Transformers, first introduced by Vaswani (2017) in 2017, have significantly advanced deep learning, particularly through the adoption of self-attention mechanisms (Ji et al., 2024). Unlike traditional models that process input data sequentially or focus on local features, Transformers can capture long-range dependencies and relationships across the entire input sequence, which is crucial for tasks like medical imaging. The self-attention mechanism, a core component of the Transformer, operates by calculating relationships between different parts of the input using three key matrices: query, key, and value. This allows the network to focus on the most relevant features, enabling it to learn complex patterns and improve performance in tasks such as image classification (Zhang et al., 2024e; Wu et al., 2024a), segmentation (Tan et al., 2024), and detection. The basic structure is shown in Fig. 7b.

Building on this architecture, the Vision Transformer (ViT) adapts the Transformer model for image analysis by dividing images into patches and treating them as a sequence. By leveraging self-attention, ViT effectively captures both global and local image features, which is particularly beneficial in medical applications like pulmonary nodule detection in CT scans. Recent studies, such as those by Hui Zhang et al. (2022a) and Chi et al. (2024), have demonstrated that incorporating Transformer-based models significantly improves detection sensitivity and reduces false positives. Chi et al. showed that integrating Transformer layers into pulmonary nodule classification tasks resulted in higher accuracy and better interpretability. Similarly, Yang et al. (2023) explored the application of uncertainty-aware attention in UGMCS-Net, further enhancing segmentation performance, particularly in complex nodule shapes and low-confidence regions.

In addition to ViT, hybrid models like the Swin Transformer have been developed to handle high-resolution medical images by introducing a hierarchical structure. This design allows the model to process images at multiple scales, capturing detailed features across different levels of granularity. For instance, Liu et al. (2024) incorporated 3D coordinate attention and edge enhancement in SCA-VNet, achieving

a high Dice coefficient by improving edge detection in pulmonary nodule segmentation. Similarly, Wang et al. (2024) utilized attention gating and multi-task learning in ExPN-Net, improving both segmentation and classification with an AUC of 0.992. These Transformer-based approaches, especially the Vision Transformer and its variants, have demonstrated significant potential in advancing the accuracy, sensitivity, and efficiency of early lung cancer detection and diagnosis.

2.6. Hybrid deep learning methods

Hybrid deep learning methods combine different types of neural networks into a unified framework to tackle complex tasks, such as pulmonary nodule detection, segmentation, and classification. By leveraging the unique strengths of various models, including CNNs, RNNs, GANs, and attention mechanisms, these hybrid methods aim to enhance overall performance, stability, and robustness. The primary advantage of hybrid models is their ability to address the limitations of individual networks, providing better feature extraction, improving accuracy, reducing false positives, and optimizing computational efficiency, particularly in challenging tasks like medical image analysis.

For example, Rashid et al. (2024) developed a framework combining local binary patterns (LBP) with Histogram of Oriented Surface Normal Vectors (HOSNV) features, achieving a sensitivity of 98.49% in detecting nodules. Cai et al. (2024a) proposed MSDet, a model that combines ERD, PCAM, and TODB to capture richer contextual information and reduce false positives caused by nodule occlusion through an extended receptive domain strategy, improving small pulmonary nodule detection and achieving an 8.8% mAP improvement on the LUNA16 dataset. Liu et al. (2020) enhanced detection robustness by incorporating adversarial attacks into CNNs, improving the system's ability to detect rare nodules under noisy conditions. Similarly, Safta and Shaffie (2024) integrated 3D-LOP descriptors with 3D-CNN features, achieving an accuracy of 97.84% and an AUC of 0.9912. As shown in Fig. 8a, Ma et al. (2024a) introduced TiCNet, combining Transformer and CNN architectures with multi-scale feature fusion, which achieved a CPM of 90.73% and a sensitivity exceeding 93%, demonstrating its efficacy in reducing false positives. These hybrid approaches show that combining diverse feature extraction and classification techniques significantly improves pulmonary nodule detection and classification accuracy.

Other studies further highlight the versatility of hybrid deep learning methods. As shown in Fig. 8b, Chi et al. (2024) and Gonidakis et al. (2023) demonstrated the effectiveness of combining local and global feature representations using attention gates and hand-crafted features, respectively. Gonidakis et al.'s method notably reduced the required training data by up to 43% while maintaining high performance. Additionally, Mao et al. (2021) employed a Hessian-MRLoG method to enhance contrast and reduce false positives, achieving a detection accuracy of 93.6%. These strategies illustrate the benefits of integrating various deep learning techniques to enhance segmentation and detection performance.

The successful applications of hybrid models, such as those proposed by Gugulothu and Balaji (2023), Usman et al. (2024), and de Pinho Pinheiro et al. (2020), highlight the effectiveness of integrating advanced algorithms to improve detection accuracy, reduce false positives, and enhance efficiency in lung cancer analysis. However, these hybrid models also introduce challenges. Their complexity can lead to overfitting, requiring additional regularization or improved generalization strategies. Furthermore, the combination of multiple components increases computational demands, leading to higher costs and longer processing times. Effectively integrating different architectures and performing hyperparameter tuning for such complex systems further adds to the difficulty. To address these challenges, more efficient model architectures, advanced optimization techniques, larger datasets, and automated hyperparameter tuning methods could be explored to improve performance and scalability.

Recently, Mamba models (Gu and Dao, 2023; Dao and Gu, 2024) have gained prominence for their ability to effectively capture long-range dependencies (Zhang et al., 2024c,b), significantly enhancing performance in dense prediction tasks like semantic segmentation. Studies by Bian et al. (2024) and Zhang et al. (2024h) have demonstrated the significant potential of the Mamba architecture in medical image segmentation through the development of the MambaClinix model and VM-UNetV2 framework. MambaClinix combines the Mamba architecture with Hierarchical Gated Convolutional Networks (HGCN), achieving an effective balance between local and global features in 3D medical images. Its lower-level modules capture high-order spatial relationships, while the higher-level modules utilize the Mamba architecture to extract long-range dependencies, resulting in remarkable segmentation performance in datasets involving lung and liver tumors. Simultaneously, VM-UNetV2 introduces a Vision State Space (VSS) model and a Semantics and Detail Infusion (SDI) module, using linear computational complexity to efficiently capture contextual information. Compared to traditional CNNs and Transformer-based models, VM-UNetV2 has demonstrated superior performance in medical segmentation tasks. This trend represents a significant advancement in intelligent medicine, particularly in medical image analysis, where hybrid models incorporating the Mamba architecture (Gu and Dao, 2023; Dao and Gu, 2024) are overcoming the limitations of traditional methods in terms of computational efficiency and global feature extraction. As the volume of medical data continues to grow, models capable of efficiently modeling long-range dependencies and handling complex contextual information will become increasingly essential. These advancements not only enhance early disease detection and diagnosis but also lay a strong foundation for the widespread adoption of intelligent medical systems.

In summary, hybrid deep learning models represent a rapidly growing trend, particularly in the field of pulmonary nodule detection and classification, where these models are showing significant potential. With ongoing advancements in deep learning technologies and the expansion of interdisciplinary research, even more innovative hybrid models are expected to emerge. These models will likely address increasingly complex challenges, driving further progress in the early detection and accurate diagnosis of lung cancer, ultimately improving clinical outcomes.

3. Literature search and screening

This review systematically retrieved relevant literature from multiple databases, including IEEE Xplore, Wiley Online Library, Google Scholar, Web of Science, ACM, Science Direct, Springer Link, and Engineering Village, covering the period from January 2020 to May 2024. The distribution of publications across these databases is shown in Fig. 9a. Through rigorous screening, this review consolidates the applications of machine learning and deep learning techniques in computer-aided diagnosis (CAD) of pulmonary nodules, with a particular focus on their implementation in CT imaging. In addition to highlighting major research achievements, this review discusses the advantages and limitations of current technologies and outlines future research directions, providing valuable insights for researchers in the field.

During the retrieval process, 406 relevant articles were identified, covering different aspects of pulmonary nodule analysis: 124 on detection, 155 on segmentation, and 127 on classification, as illustrated in Fig. 9b. After applying stringent screening criteria, 131 articles were selected, with the selection process depicted in Fig. 10. The final selection includes 56 articles on detection, 33 on segmentation, and 42 on classification. The subsequent sections will discuss the technical approaches, research outcomes, and applications derived from these studies, providing a comprehensive overview of the CAD landscape for pulmonary nodules and offering a thorough understanding of the current research status and future trends in this evolving field.

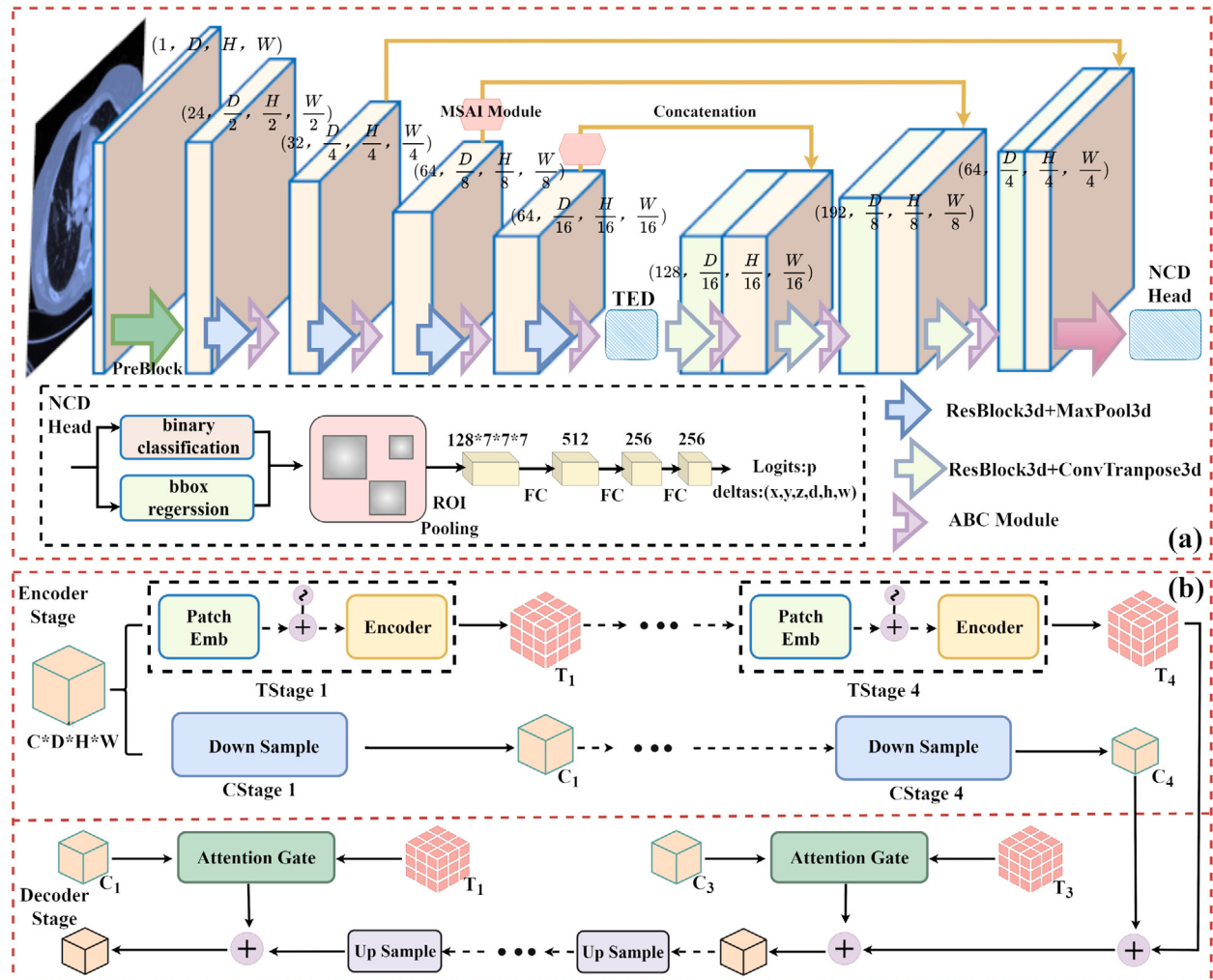


Fig. 8. Some structural examples of hybrid deep learning models: (a) Combination of 3D CNN, ACB, MSAI, TED, and dual heads for NCD and FPR (Ma et al., 2024a), which enhances multi-scale feature extraction and improves both classification and localization in nodule detection. (b) Combination of CNN and Transformer branches with attention gates for local and global feature coupling (Chi et al., 2024), allowing efficient integration of local and global features and guiding the decoding process for better feature reconstruction and detection accuracy in medical images.

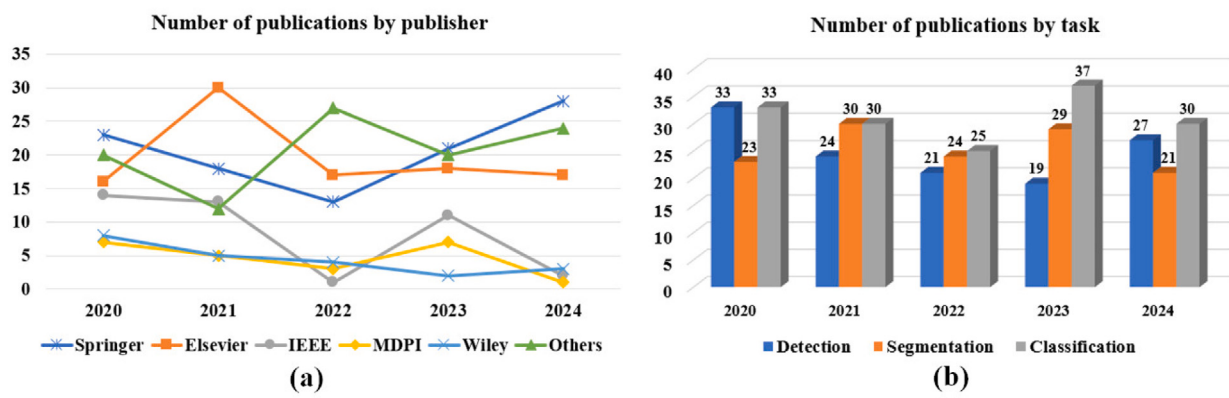


Fig. 9. (a) Number of publications in each database/platform from 2020 to 2024. (b) Number of publications on different pulmonary nodule treatment tasks from 2020 to 2024.

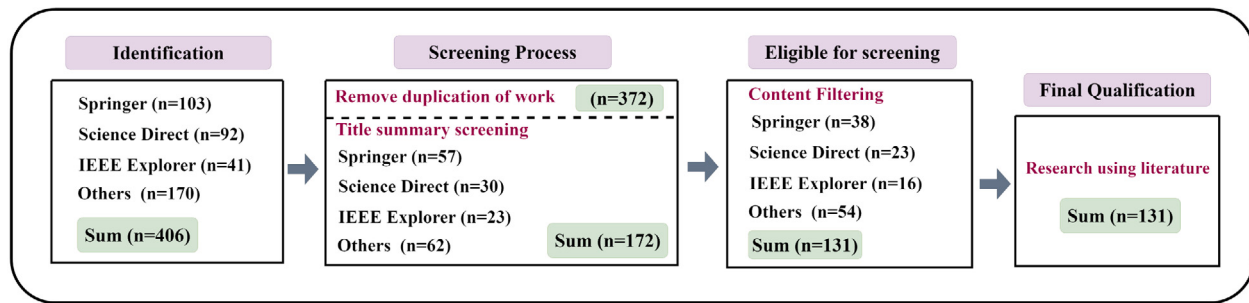


Fig. 10. The literature screening process adapted in this study. Screening criteria for step 2 include the following: time range (2020.1–2024.5), journal publication, journal type, and language (English); screening criteria for step 3 include the exclusion of methods that do not meet the criteria and conference papers. ‘Others’ includes publications from Wiley, MDPI, Taylor and Francis, and Hindawi.

4. Datasets and benchmarks

The development of Computer-Aided Diagnosis (CAD) systems for pulmonary nodules relies heavily on high-quality imaging data and robust evaluation metrics. Publicly available datasets serve as foundational resources for training, testing, and validating deep learning algorithms, facilitating standardized comparisons across different methods. These datasets vary in size, annotation quality, and imaging techniques, making them critical for different stages of research and clinical applications. In addition to datasets, benchmarks play a key role in evaluating the performance of CAD systems, providing objective metrics such as accuracy, sensitivity, and specificity to assess algorithm effectiveness. This section provides an overview of the key datasets widely used in CAD research for pulmonary nodules and discusses the most commonly employed benchmarks and evaluation metrics. As shown in Table 2, these datasets provide essential resources for advancing research in pulmonary nodule detection and diagnosis.

The LIDC-IDRI dataset (Armato et al., 2011) is one of the most comprehensive publicly available lung CT datasets, jointly created by the National Cancer Institute (NCI) and the American College of Radiology (ACR). It contains over 1,000 lung CT cases, annotated by four experienced thoracic radiologists through a multi-phase, consensus-based evaluation. Each scan is annotated with regions of interest, specifically focusing on pulmonary nodules of varying sizes, and includes both nodule and non-nodule cases. The diversity of imaging protocols and scanning devices makes this dataset widely applicable for CAD system development. Furthermore, its comprehensive annotations from different radiologists allow for the exploration of inter-observer variability, a key challenge in medical image analysis.

The LUNA16 dataset (Setio et al., 2017) is derived from LIDC-IDRI but focuses specifically on pulmonary nodule detection. It includes 888 high-quality CT scans with detailed annotations of nodules larger than 3 mm in diameter. LUNA16 also provides a standardized evaluation framework, making it a widely adopted benchmark for comparing nodule detection algorithms. The dataset includes annotations that highlight the location and size of each nodule, offering a valuable resource for both segmentation and detection tasks. The nodule cases are categorized based on their risk levels, helping researchers more effectively distinguish between benign and malignant nodules.

The ELCAP dataset (Henschke et al., 2001) is part of the Early Lung Cancer Action Project and consists of low-dose CT (LDCT) scans, primarily targeting high-risk populations, such as heavy smokers. ELCAP emphasizes early-stage lung cancer screening and includes a large number of small nodules, making it an essential resource for early detection studies. The dataset includes detailed clinical and demographic information, such as patient age, smoking history, and risk factors. Although only part of this dataset is publicly available, its focus on high-risk groups makes it valuable for developing screening algorithms aimed at detecting lung cancer in its earliest stages.

The NSCLC-Radiomics dataset (Aerts et al., 2014) focuses on non-small cell lung cancer (NSCLC) and includes not only CT scans but

also extensive clinical and molecular data. This dataset contains over 400 CT scans from patients with NSCLC, annotated with tumor regions, genomic information, and treatment outcomes. Its richness in clinical context makes it particularly valuable for research into personalized treatment strategies and prognostic modeling. The dataset also supports the study of radiomics, which involves extracting a large number of features from medical images to uncover disease characteristics that are not visible to the naked eye, providing a bridge between medical imaging and molecular biology.

The ANODE09 dataset (Van Ginneken et al., 2010) was developed for an international competition on automatic pulmonary nodule detection and consists of 55 CT scans that cover a wide range of nodule types, sizes, and shapes. This dataset focuses on providing a controlled environment for evaluating detection algorithms. The standardized evaluation metrics, such as sensitivity and false positive rates, facilitate direct comparisons between different methods. Although smaller in size compared to other datasets, ANODE09 is highly structured and provides clear, well-defined cases that are ideal for benchmarking new detection techniques. The diversity of nodule types, including solid, subsolid, and ground-glass opacities, presents an additional challenge for algorithm development, making this dataset particularly useful for testing algorithm robustness.

The PN9 dataset (Mei et al., 2021), released in 2020, is a relatively new and valuable resource for pulmonary nodule analysis. It contains high-resolution CT images collected from multiple institutions and scanners, enhancing its diversity and representativeness. One of its key strengths lies in the inclusion of subtle and diagnostically challenging nodules, which are often underrepresented in older datasets. Additionally, PN9 offers clinical annotations that are closely aligned with contemporary diagnostic standards, making it particularly suitable for training and validating models intended for real-world clinical deployment.

In terms of evaluating the effectiveness of CAD systems, several standardized benchmarks and evaluation metrics are employed. One widely adopted benchmark for nodule detection is the Competition Performance Metric (CPM), based on the Free-Response Receiver Operating Characteristic (FROC) curve. CPM evaluates an algorithm's sensitivity at predefined false positive rates, typically ranging from 1/8 to 8 false positives per scan. By averaging sensitivity at these rates, CPM provides a robust measure of how well a model balances sensitivity and false positives. The FROC curve, which plots the true positive rate (sensitivity) against the average number of false positives per scan, is a key tool in CAD research. The area under the FROC curve (AUC) indicates overall performance, with higher AUC values (ranging from 0.5 to 1) reflecting better discrimination between positive and negative cases.

For segmentation tasks, the Dice Similarity Coefficient (DSC) is commonly employed to assess how accurately an algorithm delineates nodule boundaries, with higher DSC values indicating better overlap between predicted and actual segmentations. In classification tasks, key

Table 2

Overview of datasets commonly adapted in pulmonary nodule computer-aided diagnosis (CAD) research.

Dataset	No. of scans	Focus area	Use case	Annotations
LIDC-IDRI	1018	Pulmonary nodule Detection	Detection, Classification, Segmentation	✓
LUNA16	888	Nodule Detection (Nodules >3 mm)	Detection Benchmark	✓
ELCAP	50	Early Lung Cancer Screening	Early Detection	✓
NSCLC	422	Non-Small Cell Lung Cancer	Personalized Treatment, Prognosis	✓
ANODE09	55	Nodule Detection (Various types)	Benchmarking Detection Algorithms	✓
PN9	8798	Nodule Detection & Classification	Large-scale Model Training & Validation	✓

metrics include sensitivity (the ability to correctly identify nodules), specificity (the ability to correctly identify non-nodules), and accuracy, which measures the overall correctness of the model's predictions. These metrics—sensitivity, AUC, specificity, and DSC—are critical for balancing nodule detection and minimizing false positives, ultimately guiding the development of reliable CAD systems for clinical practice.

We also conducted a detailed analysis of distributional imbalances in the two most widely used public datasets, LIDC-IDRI and LUNA16. In LIDC-IDRI, benign nodules account for 82% (3,572/4,356) of all annotated nodules, leading to a strong class skew. Gautam et al. (2024) have shown that models trained on this imbalanced distribution suffer a 12.8% drop in sensitivity when evaluated on clinical cohorts with a more realistic 45% benign-to-malignant ratio. Moreover, both datasets exhibit a size imbalance, with the vast majority of nodules falling in the 3–10 mm range and very few examples of very small or large nodules; a label imbalance, where certain subtypes (e.g., part-solid or ground-glass) are underrepresented; and an anatomical imbalance, as nodules cluster in specific lung regions. To help mitigate some of these issues, we have updated Table 2 to include the more recently released PN9 (2020) dataset, which provides a larger and more evenly distributed sample across nodule sizes, subtypes, and acquisition sources.

5. Discussion: Key techniques and breakthroughs in lung cancer detection, segmentation, and classification

In recent years, AI-driven advancements in computer-aided diagnosis (CAD) systems for pulmonary nodules have transformed the field of lung cancer detection, segmentation, and classification. These innovations, bolstered by high-quality datasets such as LIDC-IDRI and LUNA16, have not only accelerated technological progress but also fostered international research collaboration. In detection, the integration of deep learning models, especially multi-task convolutional neural networks, has significantly enhanced the sensitivity and accuracy of identifying nodules from CT scans. In segmentation, advanced models like UNet, 3D CNNs, and GANs have greatly improved precision in delineating nodule boundaries, a critical factor in evaluating nodule size and growth. For classification, the combination of deep learning techniques and texture-based features has refined the differentiation between benign and malignant nodules, thus improving diagnostic reliability. Together, these innovations have optimized CAD systems, paving the way for broader clinical applications and improved patient outcomes through earlier and more accurate lung cancer diagnoses. The following sections will examine recent progress in detection, segmentation, and classification, highlighting the key techniques and breakthroughs in each area and providing a critical analysis of their clinical relevance and future directions.

5.1. Discussion on AI-driven advances in lung cancer detection

Detecting pulmonary nodules is essential for early lung cancer diagnosis and treatment, enabling timely intervention. Pulmonary nodule detection generally involves two stages: screening potential nodules in CT scans and classifying malignancy likelihood, which guides clinical decisions. Recent advancements in AI, particularly deep learning models like multi-task CNNs, YOLOv4, UNet, and GANs, have significantly improved detection sensitivity and accuracy, enhancing CAD systems.

High-quality datasets such as LIDC-IDRI and LUNA16 have facilitated these advances by providing annotated data for effective model training. Table 3 summarizes 19 recent studies (2020–2024) utilizing the LIDC-IDRI dataset, highlighting their strengths, limitations, and clinical relevance.

Key Innovations and Performance Comparisons: Over the past several years, significant advancements have been made in AI-driven pulmonary nodule detection, contributing uniquely to the evolution of the field. In 2020, Masud et al. (2020) developed a lightweight deep learning model achieving 97.9% accuracy, showcasing the potential for AI deployment in resource-constrained environments, such as mobile devices in clinics with limited computational power. In 2022, Bhatt et al. (2022) demonstrated the utility of YOLOv4 for real-time detection with 95% precision, emphasizing the practical application of AI in rapid diagnostics. Fu et al. (2021) integrated 3D CT imaging with serum biomarkers, highlighting a multimodal approach that combines diverse data sources to enhance diagnostic precision. In 2023, Gugulothu and Balaji (2023) introduced a hybrid deep learning approach, and by 2024, Gautam et al. (2024) combined ResNet, DenseNet, and EfficientNet to achieve a sensitivity of 98.6%, significantly reducing false negatives. Furthermore, Usman et al. (2024) developed MEDS-Net, which achieved a CPM score of 93.6% by reducing false positives, thus minimizing unnecessary invasive procedures and enhancing diagnostic reliability. These innovations collectively advance the clinical applicability of AI for lung cancer detection by improving both accuracy and efficiency. To address dataset imbalances, recent studies have adopted dynamic weighted loss functions and carefully tuned oversampling strategies. Dynamic weighting—where training losses for minority classes are up-weighted on the fly—has been shown to improve recall on underrepresented nodules, reducing false negatives without destabilizing overall training. However, overly aggressive oversampling in LUNA16 can introduce synthetic bias and lead to overfitting, ultimately harming model generalization on unseen data. We therefore highlight a balanced approach: combining moderate oversampling with cost-sensitive learning and regularization techniques to narrow the generalization gap and mitigate diagnostic blind spots in real-world clinical deployments.

Model Adoption and Clinical Implications: The discussed studies highlight a range of technical approaches focusing on improving sensitivity, computational efficiency, and real-time applicability. Models such as YOLOv4 and MEDS-Net illustrate the potential of AI to be integrated into practical, real-time clinical workflows, whereas the multimodal diagnostic model by Fu et al. (2021) underscores the value of combining multiple data sources for a more comprehensive diagnostic approach. A crucial factor in clinical adoption is the computational complexity of these models. While high accuracy is desirable, the scalability of complex models like Mask R-CNN and GANs is often limited due to their heavy computational requirements. For instance, Zhu et al.'s (2021a) GAN-based approach effectively addresses data imbalance but at the cost of significant computational demands, potentially hindering scalability in less resource-rich environments. In contrast, Wu et al.'s (2024b) enhancement of YOLOv7 presents a more efficient model that balances performance and computational load, making it more practical for broader clinical implementation.

Comparisons Across Benchmark Datasets: Compared to the LIDC-IDRI dataset, LUNA16 employs CPM (Competition Performance Metric)

Table 3

Pulmonary nodule detection methods and their performance in CT images from the LIDC-IDRI dataset.

Authors	Year	2D/3D	Technique/ Network Type	Training/ Validation/ Testing Set	Software/ Hardware Utilized	Main Method	Nodules Types	Validation/ Test Method	Model Performance
Veronica (2020)	2020	2D and 3D	ANN, Fuzzy C-Means	LIDC-IDRI, ELCAP	MATLAB, 4GB RAM	FCM, ANN with OALO	Benign, malignant	Sensitivity: 96.10%	
Bhatt et al. (2022)	2022	2D	YOLOv4	Tra 70%, Val 20%, Test 10%	TensorFlow RTX 2070	YOLOv4 model	Various nodule types and sizes	YOLOv4: 81.00%	
Harsono et al. (2022)	2022	3D	I3DR-Net	LIDC: 605 tra, 202 val, 202 tes	Pytorch, Tesla P100 16GB	Inflated 3D ConvNet (I3D)	Solid and non-solid nodules	Sensitivity: 94.60%	
Nair et al. (2022)	2022	2D	RWI segmentation, RF, KNN	534 training, 150 testing	MATLAB 2018a	Random Walker with Random Forest, k-NN	Benign and malignant nodules	RWI-RF: 99.99%; RWI-k-NN: 98.991%	
Jain et al. (2023)	2023	3D	Two-stage CNN, U-net	LIDC-IDRI: 5023tra/val	Python, Tesla P100	Two-stage CNN, U-net	Pulmonary nodules \geq 3 mm	Train-Validation-Test Split	Sensitivity: 83.55%
Gugulothu and Balaji (2023)	2023	2D	CSDR-J-WHGAN	Training 80%, Testing 20%	Python	SDMMT, MD-HHOA, CSDR-J-WHGAN	Nodule and non-nodule	Sensitivity: 96.98%	
Rashid et al. (2024)	2024	2D and 3D	HOSNV, LBP, XGBoost	LIDC-IDRI	–	XGBoost	Vessel, isolated, juxtapleural	XGBoost: 98.49%	
Agnes et al. (2024)	2024	2D	Wavelet U-Net++	LIDC-IDRI: 1018 scans	Python Keras, GPU	U-Net++, hybrid loss	Small, irregular nodules	DSC: 93.70%; IoU: 87.80%	
Gautam et al. (2024)	2024	2D	ResNet-152, EfficientNet-B7	LIDC-IDRI	–	Weighted average ensemble	Benign and malignant	Sensitivity: 98.60%	
Gugulothu and Balaji (2024)	2024	2D	Hybrid DL (HDE-NN)	LIDC-IDRI	–	Hybrid differential evolution-based NN	Benign and malignant	Sensitivity: 95.25%	
Halder et al. (2020)	2020	2D	Segmentation (AMST)	LIDC-IDRI, private dataset	–	Morphological filter with SVM	Solid, subsolid, GGO	Sensitivity: 94.88%	
Masud et al. (2020)	2020	2D	CNN	LIDC 1279 images	Nvidia GTX1050, 12GB	Light CNN	Normal, Benign, malignant	Accuracy: 97.90%	
Farhangi et al. (2021)	2021	2D and 3D	Unified CNN	888 CT exams	CT volume: 12 min	Dilated 1D convolutions	Solid, subsolid, large nodules	10-fold cross-validation	Sensitivity: >96.00%
Zheng et al. (2021)	2021	3D	U-net++, Efficient-Net	LIDC: 888scans, 1186 nodules	–	Multiscale dense CNNs	Small nodules (<6 mm)	Sensitivity: 94.20%	
Chen et al. (2023)	2022	3D	F-Net, MSS-Net	Training 70%, Validation 20%, Test 10%	–	F-Net, MSS-Net	Solitary, varying sizes (3–30 mm)	0.971 (1 FP/scan); 0.978 (2 FPs/scan)	
Usman et al. (2024)	2024	3D	Multi-encoder, Self-distillation	Training 80%, Validation 10%	Python	3Dsub-volumes, self-distillation	Nodules \geq 3 mm	20.27 Fps/scan	
Fu et al. (2021)	2021	3D	Multi-DL, MLP	3:1 training/validation	Keras, GTX1080ti	Fusion of 3D lung CT images	Squamous cell carcinoma	Specificity: 90.60%	
Majidpourkhoei et al. (2021)	2021	3D	CNN	LIDC, 1415 test images	Python, 8GB RAM	CNN with 3D convolutions	Nodule sizes (1–5 mm)	5-fold cross-validation	Specificity: 91.70%
Hung et al. (2023)	2023	3D	HSNet	Original: 4252 images, split 3:1	TensorFlow 2.7, NVIDIA RTX 3060, 32GB	3D hierarchical semantic CNN (HSNet)	Subtlety, texture, sphericity, malignancy	Cal: 98.73%; Margin: 92.07%; Subtlety: 90.26%	

as a benchmark, providing a standardized measure for comparing CAD system performance. This allows for a clearer evaluation of different models' strengths and applicability in various clinical scenarios. **Table 4** compiles key metrics such as author, year, technique type, validation method, and CPM score, offering a comprehensive view of advancements between 2020 and 2024. Studies employing deep learning techniques that integrate 3D contextual information and multi-scale feature fusion, such as Mask R-CNN and 3D CPM-Net, exhibit outstanding performance, improving detection accuracy while minimizing false positives.

Future Directions and Clinical Potential: The development and adoption of AI-driven CAD systems for pulmonary nodule detection must prioritize clinical integration and adaptability. Future research should focus on reducing computational complexity to make these models suitable for environments with limited resources, further developing lightweight and real-time applications to expand access, and integrating multimodal data, such as combining imaging with biomarkers, to improve diagnostic precision. In conclusion, advancements in AI-driven pulmonary nodule detection have significantly enhanced detection sensitivity, reduced false positives, and improved clinical applicability, paving the way for broader adoption. Successful integration into clinical practice, with a continued emphasis on balancing efficiency and accuracy, is essential for realizing the full impact of these systems on patient care.

Single-Stage Detectors for Real-Time Nodule Analysis: Single-stage object detectors such as YOLO-v5 and YOLO-v6 have emerged as powerful tools that balance high detection accuracy with real-time inference, making them ideally suited for integration into clinical workflows. YOLO-v5 bypasses the region-proposal stage by predicting bounding boxes and class probabilities in a single network pass; for

instance, Ahmadyar et al. (2024) combined a hierarchical YOLO-v5s with a 3D CNN backbone on LUNA16, achieving 97.8% sensitivity at a 0.3 confidence threshold (Ahmadyar et al., 2024). Wu et al. (2024) further refined this framework with their YOLO-MSRF variant—incorporating multi-scale feature refinement—to reach 94.02% sensitivity and 95.26% mAP on the same benchmark (Wu et al., 2024b). YOLO-v6 further advances the architecture by employing an optimized backbone and anchor-free detection head to reduce latency and enhance small-object recall—key for identifying subtle or diminutive nodules—and early reports indicate over 98% sensitivity on LIDC-IDRI with per-slice inference times under 50 ms. These developments underscore a trend toward embedding lightweight, fast, and accurate CAD tools directly within PACS or imaging consoles, thereby broadening access to AI-driven lung cancer screening in routine clinical practice.

5.2. Discussion on AI-driven advances in lung cancer segmentation

Pulmonary nodule segmentation is vital for early lung cancer diagnosis, involving the precise identification of nodules in CT images for volumetric analysis, growth rate estimation, and characterization—critical for treatment strategies. Segmentation quality directly impacts clinical decisions, making it essential for CAD systems. Recent AI advancements, particularly in deep learning models like UNet, GANs, and 3D CNNs, have enhanced segmentation accuracy, supported by datasets such as LIDC-IDRI and LUNA16. **Table 5** summarizes recent studies, detailing model performance, datasets, and validation methods, helping identify suitable models for clinical use. Ultimately, improved segmentation accuracy supports early diagnosis, treatment planning, and better patient outcomes.

Table 4

Pulmonary nodule detection methods and their performance in CT images from the LUNA16 dataset.

Authors	Year	2D/3D	Technique/ Network Type	Training/ Validation/ Testing Set	Software/ Hardware Utilized	Main Method	Nodules Types	Validation/ Test Method	Model Performance
Cai et al. (2020)	2020	3D	Mask R-CNN	LUNA16, Ali TianChi	Quadro P6000 GPU	Mask R-CNN, ResNet50, FPN, RPN	Benign and malignant		88.1% at 1 FP/scan; 88.7% at 4 FP/scan; AP@50: 88.2%
Song et al. (2020)	2020	3D	3D CPM-Net	LUNA16 (888 scans)	SenseCare Platform	Anchor-free, 3D context	Benign and malignant		91.2% at 1 FP/scan; 92.4% at 2 FP/scan
Yuan et al. (2021)	2021	3D	Multi-path 3D CNN	LUNA16, split 8:1:1	TensorFlow, RTX2080 TI GPU	Multi-path 3D CNN, feature fusion	Various sizes		0.952 at 4 FP/scan; 0.962 at 8 FP/scan; CPM: 0.881
Agnes et al. (2022)	2022	2D and 3D	Two-stage Pulmonary nodule detection	23,720 CT, 80% Train, 20% Test	Keras, GTX 1060 (6 GB)	Atrous UNet+, PD-CLSTM	Small nodules (5–9 mm)		0.544–0.986 at different FP levels; CPM: 0.93
Zhao et al. (2022)	2022	2D and 3D	Faster R-CNN	LUNA16	Platform - Colab; Ubuntu; K80 GPU	Multiscale fusion	Small nodules	Train- Validation-Test Split	0.905 at 4 FP/scan; CPM: 0.829
Gonidakis et al. (2023)	2023	3D	Handcrafted features + CNN	70% Train, 10% Val, 20% Test	Keras with TensorFlow, 2080 RX	Handcrafted + CNN	Benign and malignant		0.5 mean FP/scan; Fusion: 94.3%
Hendrix et al. (2023)	2023	2D and 3D	AI system	500 CT (Hospital A), 888 (LUNA16)	–	AI, multi-view ResNet50, FROC	Actionable benign nodules		Internal: 90.9%; External: 92.4%; Benign: 94.3%
Wu et al. (2024b)	2024	2D	YOLO-MSRF	LUNA16	–	YOLO-MSRF	Benign and malignant		Sensitivity: 94.02%; mAP: 95.26%
Zhang et al. (2024)	2024	3D	S-Net, U-shaped	LUNA16	–	S-Net, hybrid loss	Different shapes		S-Net(R): 0.914; S-Net(S): 0.915
Budati and Karumuri (2024)	2024	2D	SbYSF, Sailfish + YOLO	LUNA16	Python in Windows 10	Sailfish-based YOLO (SbYSF)	Lung cancer nodules		CPM: 99.75%
Cao et al. (2020)	2020	3D	Two-Stage CNN	LUNA16, 10% validation	Ubuntu 14.04, Python 3.6.4, GTx-1080Ti	TSCNN: UNet, 3D CNN	Calcific, cavitory		DenseNet: 0.768; SeResNet: 0.730; IncepNet: 0.686
Zhu et al. (2021a)	2021	3D	FRGAN	543 images, augmented to 0.22M	Adam optimizer, learning rate 1.0×10^{-4}	GAN augmentation, 3D-CNN	Solid, subsolid, large nodules		CPM: 0.915
Shi et al. (2021)	2021	3D	3D Res-I, Faster R-CNN	Fold 1–9 Train, Fold 0 Test	Ubuntu 16.04, PyTorch, GTx 1080Ti	U-Net-Like network, Faster R-CNN	Solid, semi-solid		Sensitivity: 96.37%; FROC: 83.75%
Zhang et al. (2022a)	2022	3D	3D MSA, 3D Faster R-CNN	LUNA16, TianChi	–	Multiscale attention	Various sizes	10-fold cross- validation	0.945 at 1 FP/scan; CPM: 0.927
Zhang and Zhang (2023)	2023	3D	LungSeek, 3D SK-ResNet	LUNA16: 9 Train subsets (800 CT)	PyTorch, GTx 1080, 16 GB RAM	LungSeek, 3D SK-ResNet	Benign and malignant		SK-ResNet: 95.78%; Res18: 95.53%; DPN: 94.32%
Gao et al. (2024)	2024	3D	FULFIL, GCN	LUNA: 140 scans	PyTorch 1.1.0, RTX 3090	FULFIL, GCN, Teacher-Student	Benign and malignant		0.574 at 0.125 FP/scan
Lin et al. (2024b)	2024	3D	3D RPN	LUNA16, LNOP, LNHE	PyTorch, RTX 2070, 24GB RAM	Modified 3D RPN, CSP-ResNeXt, FPN	Different solid		96.6% at 8 FP/scan for LUNA16; CPM: 90.10%

Key Innovations and Performance Comparisons: Recent AI-driven advancements in pulmonary nodule segmentation have significantly enhanced both accuracy and clinical utility. In 2020, Chen et al. (2020) introduced the LDDNet model, achieving over 99% segmentation accuracy on the LIDC-IDRI dataset, showing strong potential for reducing manual workload and improving consistency in clinical nodule identification. Khanna et al. (2020) similarly demonstrated the robustness of deep learning approaches with their deep residual U-Net, reaching a Dice Similarity Coefficient (DSC) of over 98% on the LUNA16 dataset. In 2021, Dutande et al. (2021) and Kadia et al. (2021) presented a 2D–3D cascaded CNN and the R2U3D model, respectively, emphasizing the benefits of using multiple dimensionalities for capturing diverse features in nodule segmentation. In 2022, Zhang et al. (2022b) introduced the I-3D DenseUNet, excelling in segmenting complex tumor shapes, while Tyagi and Talbar (2022) leveraged a CSE-GAN to overcome challenges posed by data scarcity, a common issue in medical imaging. Recent models have also focused on hybrid and multi-modal approaches: in 2023, Youssef et al. (2023) combined deep learning with stochastic models for enhanced robustness, while Nguyen et al. (2023) used a multi-branch attention mechanism to improve segmentation accuracy. In 2024, Bbosa et al. (2024) and Sweetline et al. (2024) developed MRUNet-3D and a multi-crop CNN, respectively, both demonstrating strong performance in segmenting small nodules—critical for the early detection necessary for effective lung cancer treatment.

Performance Evaluation via Dice Similarity Coefficient (DSC): Recent studies indicate significant progress in deep learning-based pulmonary nodule segmentation, particularly regarding the Dice Similarity Coefficient (DSC). Halder et al. (2020) achieved a sensitivity of 94.88%

on the LIDC-IDRI dataset. Chen et al. (2020) introduced LDDNet, which recorded over 99% accuracy in lung parenchyma segmentation. Zhang et al. (2022b) reported an 83.16% DSC with their I-3D DenseUNet on the LIDC dataset, while Liu et al. (2024) reached a DSC of 87.50% with their SCA-VNet on the LIDC-IDRI dataset. Sweetline et al. (2024) developed a multi-crop CNN that achieved accuracies of 98.3% and 98.5% on the LUNA16 and LIDC-IDRI datasets, respectively. These advances, primarily based on U-Net variants, CNNs, and attention mechanisms, have significantly improved segmentation accuracy and reliability.

Model Adoption and Clinical Implications: The successful adoption of AI-driven segmentation models in clinical settings hinges on balancing accuracy with computational efficiency. While high-performing models like LDDNet and deep residual U-Net show great promise due to their high accuracy, they also present computational challenges that can hinder scalability, especially in resource-limited healthcare facilities. For instance, Zhang et al.'s (2022b) I-3D DenseUNet demonstrated excellent segmentation accuracy but may not be feasible for smaller healthcare centers due to its high computational demands. In contrast, Liu et al.'s (2024) SCA-VNet offers a more balanced approach, achieving a DSC of 87.5% while minimizing computational overhead, making it a more practical candidate for widespread clinical adoption. Additionally, reducing false positives remains a critical aspect of clinical deployment, as minimizing unnecessary procedures is vital for patient safety and healthcare efficiency. Approaches like attention mechanisms and ensemble learning, utilized in models such as MANet and SCA-VNet, enhance precision and sensitivity, ultimately making these models more reliable and suitable for real-world clinical use.

Future Directions and Clinical Potential: Future research in AI-driven pulmonary nodule segmentation should prioritize developing

Table 5

Methods and their performance in pulmonary nodule segmentation on CT images.

Authors	Year	Dataset	Technique/ Network Type	Main Method	Software/ Hardware Utilized	Validation/ Test Method	Model Performance
Dutande et al. (2021)	2021	LIDC-IDRI, LNDb, ILCID	2D–3D cascaded CNN	SquExUNet: Segmentation	Keras, NVIDIA P100 16GB		Segmentation: 80.00%; Detection: 90.01%
Kadia et al. (2021)	2021	LUNA16, VESSEL12	R2U3D	R2U3D with 3D convolution.	Keras, NVIDIA RTX 2080 Ti		Soft-DSC: 0.9920
Liu et al. (2024)	2024	LIDC-IDRI	SCA-VNet	Residual edge enhancement	PyTorch 1.12.1		DSC: 87.50%; Sensitivity: 86.80%; Precision: 88.32%
Agnes et al. (2024)	2024	LIDC-IDRI	Wavelet U-Net++	U-Net++ with wavelet pooling	Python Keras, GPU		DSC: 93.7% ± 0.14
Cai et al. (2020)	2020	LUNA16, TianChi	Mask R-CNN	Mask R-CNN, resnet50 backbone	Quadro p6000 (1.08GB)		88.1% at 1 false positive/scan; 88.7% at 4 false positives/scan
Osadebey et al. (2021)	2021	LIDC-IDRI, 3DIRCAD, ILD, PHTM	CNNs and U-net	Preprocessing: CNN classifier; Processing: U-net	MATLAB, Windows 10, Intel i7-8650U	Train- Validation-Test Split	3DIRCAD: 0.76–0.95; ILD: 0.81–0.95
Zhu et al. (2021b)	2021	LUNA16	HR-MPF	HR-MPF with PDM	PyTorch, Intel i7-10700, GTX 2070		DSC: 0.9373; Sensitivity: 0.9377; Precision: 0.9427
Tyagi and Talbar (2022)	2022	LUNA16, ILND	3D GAN	CSE-GAN with U-Net	TensorFlow, NVIDIA P100		LUNA: 80.74%, ILND: 76.36%; LUNA: 85.46%, ILND: 82.56%
Tang et al. (2023a)	2023	LUNA16	NoduleNet	AI-based CT nodule diagnosis, Lung-RADS, PCA.	PyTorch, Nvidia GTX 1060 6GB		non-solid: 0.86; partially solid: 0.68; solid: 0.94; Class 1: 0.84, Class 3: 0.29, Class 5: 0.99
Luo et al. (2024)	2024	LUNA16	RkcU-Net	Improved residual block	PyTorch, Python, NVIDIA P100		DSC: 89.25%; Sensitivity: 88.48%; Precision: 90.04%
Bbosa et al. (2024)	2024	LUNA16	MRUNet-3D	MRUNet-3D: Multi-stride	PyTorch, NVIDIA 3060		DSC: 83.47%; Sensitivity: 83.39%; Precision: 86.04%
Qiu et al. (2023)	2023	LIDC-IDRI, LUNA16	Dual-task 3D U-Net	Dual-task region-boundary	PyTorch, NVIDIA RTX 3090		LIDC-IDRI: 82.48 ± 8.17; LUNA16: 71.61 ± 14.17
Thangavel and Palanichamy (2024)	2024	LIDC-IDRI, LUNA16	T-Net, NASNet	T-Net, CenterNet, NASNet for seg	Keras, NVIDIA 98.16 mx		LIDC-IDRI: 99.07; LUNA16: 98.97
Chen et al. (2020)	2020	LIDC-IDRI	LDNet	LDNet: Uses dense block, BN	PYDICOM, CV2 (OpenCV); 32GB		Accuracy: Over 99%; High segmentation accuracy and robustness
Ni et al. (2022)	2022	LIDC-IDRI	Two-stage multitask U-Net	Coarse-to-fine 2-stage with 3D U-Net, MSU-Net.	PyTorch, 3 NVIDIA GTX-1080 GPUs		Malignancy: 83.4%; Margin: 81.4%; Calcification: 92.4%; Accuracy: 77.8%; AUC 84.3%
Zhang et al. (2022b)	2022	LIDC- IDRI, TCIA, SHATMU	I-3D DenseUNet	Nested dense skip connection, TPS augmentation.	Keras/ TensorFlow, Linux, 6 NVIDIA 12GB		TCIA/LIDC: 0.8316, SHATMU: 0.8167; TCIA/LIDC: 0.9278, SHATMU: 0.9015
Usman et al. (2023)	2023	LIDC-IDRI	MESAHA-Net	Multi-encoder structure	TensorFlow 2.0, NVIDIA	5-fold cross- validation	88.27% ± 7.42%; 92.88% ± 9.54%; 86.95% ± 11.29%
Youssef et al. (2023)	2023	LIDC-IDRI	3D U-Net	MGRF model; 3D U-Net for precise ROI segmentation.	PyTorch, Tesla V100 GPU (16GB)		Dice score: 93.64% ± 5.20%; 93.30% ± 0.72%
Khanna et al. (2020)	2020	LUNA16, VESSEL12, HUG-ILD	Deep Residual U-Net	Residual U-Net, false-positive removal.	Keras/ Tensorflow, Intel i7, GTX 1060 (6GB)		LUNA16: 98.63%; VESSEL12: 99.62%; HUG-ILD: 98.68%
Nguyen et al. (2023)	2023	LIDC-IDRI, LUNA16	3D UNet	UNet-based backbone, multi-branch attention.	NVIDIA Tesla P100 (16GB)		Consensus 3: 82.74 ± 8.11; Consensus 4: 83.61 ± 7.01; FROC sensitivity: 88.11%
Halder et al. (2020)	2020	LIDC-IDRI	AMST	ASE: Adaptive filter, reduces false positives.	Siemens Somatom Spirit scanner		Min 0.9433; Max 0.9919; Avg 0.9872; 8–9 mm: 92.90%; 9–10 mm: 93.55%; 10–20 mm: 95.83%
Bhattacharyya et al. (2023)	2023	LUNA16	DB-NET	DB-NET: Mish activation	PyTorch, NVIDIA GPU	10-fold cross- validation	DSC: 88.89%; Sensitivity: 90.24%; Precision: 77.92%
Ma et al. (2024b)	2024	LUNA16, LNDb	Dig-CS-VNet	Dig-CS-VNet: Pixel threshold	PyTorch 1.7.0, RTX A5000 × 2		LUNA16: 94.9%, LNDb: 81.1%; LUNA16: 92.7%, LNDb: 76.9%

lightweight, computationally efficient models suitable for real-time use, especially in resource-limited settings. Such advancements could support integration into mobile devices or clinical workflows, improving access to diagnostic tools in underserved areas. Moreover, integrating segmentation models with other modalities, such as imaging, biomarkers, or genomic data, could enhance diagnostic accuracy and provide a comprehensive understanding of patient conditions. In conclusion, strides in AI-driven segmentation have improved accuracy and early lung cancer detection. Successful clinical integration will require balancing performance with practical deployment, focusing on efficiency, accessibility, and multimodal data to maximize impact on patient outcomes.

5.3. Discussion on AI-driven advances in lung cancer classification

Pulmonary nodule classification aims to distinguish between benign and malignant nodules and differentiate true nodules from imaging artifacts, which is crucial for guiding clinical decisions and reducing unnecessary interventions. Recent advancements in AI have significantly improved classification accuracy, enhancing patient care and resource utilization. To summarize these advancements, we reviewed 32 studies from 2020 to 2024, encompassing machine learning, deep learning, and hybrid approaches using datasets like LIDC-IDRI and LUNA16. Table 6 highlights these studies, emphasizing their methodologies, strengths, limitations, and clinical relevance.

Table 6
Methods and their performance in pulmonary nodule classification on CT images.

Authors	Year	Dataset	Classification	Technique/ Network Type	Main Method	Software/ Hardware Utilized	Validation/ Test Method	Model Performance
Savitha and Jidesh (2020)	2020	LIDC-IDRI	Nodule or non-nodule	DCNN +CRF	DCNN + CRF for extraction and classification	i5-7300-HQ, 16GB, GTX 1050		ACC: Without CRF: 83%; With CRF: 89.48%
Naqi et al. (2020)	2020	LIDC-IDRI	Nodule or non-nodule	FODPSO; Geometric fit	Four phases: extraction, cla	MATLAB, Xeon 3.5 GHz		ACC: 96.90%; SEN: 95.60%; SPE: 97.00%
de Pinho Pinheiro et al. (2020)	2020	LIDC-IDRI	Nodule or non-nodule	CNNs	Swarm AI for CNN training	–		ACC: 93.71%; SEN: 92.96%; SPE: 98.52%
Wang et al. (2021)	2021	LIDC-IDRI	Nodule or non-nodule	CS-LBP, ORT-EOH; H-SVMs	3D feature extraction: CS-LBP, ORT-EOH	MATLAB, Xeon 3.5 GHz	Average1: 96.04%; Average2: 95.69%; Average3: 96.95%	
Naveen et al. (2023)	2023	LIDC-IDRI	Nodule or non-nodule	DS, RF, BPNN	DS, RF, BPNN for classification	–		solid: 98.00%; part-solid: 93.68%; non-solid: 97.20%
Gugulothu and Balaji (2023)	2023	LIDC-IDRI	Nodule or non-nodule	SDMMT; U-Net;TrP	Clas: CSDR-J-WHGAN	Python		CSDR-J-WHGAN: 97.11%; GAN: 95.56%; DCNN: 91.54%
Chen et al. (2021)	2021	LUNA16; Kaggle DSB	Nodule or non-nodule	LDNNET: Dense-Block, BN, Dropout	LDNNET, Dense-Block: classification	32GB RAM, 2.5 GHz CPU, GT 640M		LUNA16: 98.84%; Kaggle DSB 2017: 99.95%
Halder and Dey (2023)	2023	LIDC-IDRI	benign or Malignant	Atrous CNN: ATCNN1P, ATCNN2PR	VGG-like structure: classification	GPU in Google Colab Pro		ATCNN2PR-1: 95.97%; ATCNN2PR-2: 95.84%; ATCNN2PR-3: 96.89%
Sengodan et al. (2023)	2023	LIDC-IDRI	benign or Malignant	RCNN, Ensemble SVM	Ensemble SVM: classification	MATLAB, i7, 4 GB GPU	Train–Validation–Test Split	ACC: 98.53%; SEN: 99.30%; AUC: 0.98; SPE: 98.03%
Guo et al. (2023)	2023	LUNA16	benign or Malignant	3D SAACNet + GBM	SAACNet + GBM: extraction and classification	PyTorch, 4 GTX 2080Ti		ACC: 95.18%; SEN: 97.35%; AUC: 97.70%; SPE: 90.43%
Sivakumar et al. (2024)	2024	LUNA16, Kaggle DSB	benign or Malignant	ADBN, LightGBM	LightGBM: classification	TensorFlow, 16GB RAM		ACC: 99.87%; SEN: 99.75%; SPE: 99.42%
Zhang et al. (2021)	2021	Internal: 532pts	benign or Malignant	3D CNN, SE-ResNet	3D CNN: NSNs classification	TensorFlow, TITAN XP		AIS vs MIA-IAC: 81.9% (CNN), 86.4% (CNN + radio)
Harsono et al. (2022)	2022	LIDC-IDRI; Moscow	benign or Malignant	I3DR-Net	Transfer learning: I3D backbone, RetinaNet	PyTorch, Windows, Tesla P100		Public-1: 94.12%; Private-1: 65.90%; Public-2: 81.84%; Private-2: 70.36%
Zhang and Meng (2022)	2022	LIDC-IDRI	Both	VGG16	Seg: RW; Class: VGG16 + fused features	–		single VGG16: 0.930; multi VGG16: 0.975; multi-feature VGG16: 0.9681
Cai et al. (2023)	2023	LIDC-IDRI; HB; XZ	Both	3D MaskRCNN, ResNet18-3D	Baseline models fine-tuned with local datasets	–		LIDC baseline: 0.846; HB: 0.813; XZ: 0.696; LIDC baseline: 0.837; HB: 0.849
Gugulothu and Balaji (2024)	2024	LIDC-IDRI	Both	CBSO; IFB; HDE-NN	Seg: CBSO; Classification: HDE-NN	Keras, 32 GB RAM, i5		HDE-NN: 96.39%; SVM: 91.68%; ELM: 94.57%; HDE-NN: 95.25%; SVM: 88.38%
Raza et al. (2023)	2023	IQ-OTH/NCCD	Both	EfficientNetB1	Transfer learning: EfficientNet: class	Keras, TensorFlow; Tesla T4		No augmentation: 98.64%; With augmentation: 99.10%
Dodia et al. (2022)	2022	LUNA16	Nodule or non-nodule	RFR V-Net; NCNet	RFR V-Net: seg; NCNet: class	Keras; HPC setup		NCNet 3D: 98.21%; NCNet 3D: 98.38%; NCNet 3D: 98.33%
Lei et al. (2020)	2020	LIDC-IDRI	benign or Malignant	CNN, SAM, HESAM	SAM for shape & margin analysis	PyTorch; 2 GTX 1080 Ti		HESAM: 99.13%; SAM: 98.25%; CAM: 96.51%
Blanc et al. (2020)	2020	SFR Data Challenge 2019	Nodule or non-nodule	3D U-NET; 3D Retina-UNET;SVM	SVM: classification	IBM Power AC922, Volta V100 GPU		(95% CI: 84.83%–91.03%); AUROC: 0.9058
Fu et al. (2021)	2021	LIDC-CISB	benign or Malignant	3D multi-classification; MLP	Mr-Mc and MLP for pathological types	Keras; Dual GTX1080ti (11GB)		Mr-Mc: 0.810; MLP: 0.887; Fusion: 0.906; Mr-Mc: 0.876; MLP: 0.980; Fusion: 0.950
Amini et al. (2024)	2024	LIDC-IDRI; SPIE	benign or Malignant	FIG method	FIG for classification	–		Sub-band D2: 67.11%; 8-orientation Gabor: 70.22%
Wang et al. (2024)	2024	LIDC-IDRI; Nanjing Univ.	benign or Malignant	Multi-task DL;3D nnU-Net; AAG and SAM	3D nnU-Net: seg; ExpN-Net, AAG, SAM: classification	PyTorch, GPU	5-fold cross-validation	LIDC: 95.5%; In-house: 90.1%; LIDC: 100%; In-house: 90.9%; LIDC: 0.992; In-house: 0.923
Muzammil et al. (2021)	2021	LUNA16	benign or Malignant	DCNN + SVM + AdaBoostM2	Fusion: AlexNet, VGG-16, VGG-19	MATLAB, i7-8550U, 8GB RAM		SVM + deep: 95.59% ± 0.27%; AdaBoostM2 + deep: 95.25%
Wang et al. (2020)	2020	LIDC-IDRI, LNUTCM	benign or Malignant	EOH, MSPLBP, NNCS	Seg:EOH, MSPLBP; DLSR (Class)	MATLAB, i7, 8GB RAM		ACC: 95.88%; AUC: 0.8149 (PR curves)
Wu et al. (2023a)	2023	LIDC-IDRI; CQUCH	benign or Malignant	STLF-VA, 3D CNN	STLF-VA with self-supervised learning	Keras, Ubuntu, RTX TITAN		ACC: 85.30%; SEN: 86.80%; AUC: 0.9042; SPE: 83.90%
Lin et al. (2020)	2020	LIDC-IDRI; UCLA	Both	RetinaNet, ResNet 34, HSCNN	RetinaNet for detection; HSCNN for classification	PyTorch, Tesla V100		Diameter, consistency, margin: 0.59, 0.74, 0.75; Mean AUC for malignancy: 0.89

(continued on next page)

Table 6 (continued).

Authors	Year	Dataset	Classification	Technique/ Network Type	Main Method	Software/ Hardware Utilized	Validation/ Test Method	Model Performance
Zhang et al. (2022c)	2022	LIDC-IDRI	Nodule or non-nodule	Radiomics; ML	Various models: classification	Python, CPU, GT 640M	RF + RFE: 0.9580; Best classifier (RF + RFE): 0.9893	
Suresh and Mohan (2022)	2022	LIDC-IDRI	benign or Malignant	DCNN	Non-cancerous, malignant classification	MATLAB 2018b; GTX 960, 8 GB	ACC: 97.80%; SEN: 97.10%; AUC: 0.9956; SPE: 97.20%	
Gupta et al. (2024)	2024	LIDC-IDRI	benign or Malignant	SVM; LDA, KNN	Feature extraction: radiomics	MATLAB	10-fold cross-validation	ACC: 91.3%; SEN: 90.0%; AUC: 0.96; SPE: 92.0%
Zhai et al. (2020)	2020	LIDC-IDRI, LUNA16	benign or Malignant	Multi-task CNN (MT-CNN)	MT-CNN for classification and reconstruction	PyTorch 1.3, Tesla V100, Python 3.7		LUNA-16: 97.3%; LIDC-IDRI: 95.59%
Siddiqui et al. (2023)	2023	LIDC, LUNA16	benign or Malignant	DBN, Gabor	Gabor filters with enhanced DBN	TensorFlow, 16 GB RAM		GF-DBN-SVM: 97.877%; IGF-EDBN-SVM: 99.424%

Key Innovations and Performance Comparisons: Recent studies in pulmonary nodule classification have made significant strides in both model performance and clinical applicability. In the nodule versus non-nodule classification task, Savitha and Jidesh (2020) used a Deep Convolutional Neural Network (DCNN) combined with Conditional Random Fields (CRF) to reduce false positives, achieving a mean Intersection over Union (MIoU) of 0.911 and pixel accuracy of 89.48% on the LIDC-IDRI dataset, with precision and recall of 0.95 each. Similarly, Naqi et al. (2020) utilized geometric fitting combined with deep learning, which reduced false positives to 2.8 with a sensitivity of 95.6%, showcasing effective false positive control. de Pinho Pinheiro et al. (2020) integrated swarm intelligence algorithms with CNNs to achieve 93.71% accuracy on the LIDC-IDRI dataset, reducing training time by 25%. Wang et al. (2021) improved multi-class nodule detection using 3D texture and edge features, reaching a sensitivity of 95.69% and specificity of 96.95%. Dodia et al.'s (2022) NCNet, combining V-Net and SqueezeNet, further enhanced sensitivity to 98.38% while effectively managing false positives. These advancements highlight the diverse innovations targeting both high classification accuracy and the reduction of false positives, enhancing clinical decision-making capabilities.

In the benign versus malignant classification task, several methodologies have also emerged. Lei et al. (2020) utilized SAM and HESAM methods for shape and edge analysis to reduce false positives. Amini et al. (2024) leveraged fuzzy information and texture features, achieving high accuracy, though with slightly lower sensitivity. Suresh and Mohan (2022) achieved 97.8% accuracy using a DCNN while managing false positives effectively, and Gupta et al. (2024) demonstrated that SVM models achieved 91.3% accuracy on the LIDC-IDRI dataset. Zhai et al. (2020) used a Multi-task Convolutional Neural Network (MT-CNN) to reach an AUC of 97.3% on the LUNA16 dataset, successfully reducing false positives. Similarly, Rahouma et al. (2024) designed a genetic algorithm to optimize a 3D CNN, achieving 95.977% accuracy, while Sivakumar et al. (2024) demonstrated the potential of optimization algorithms with an accuracy of 99.87%. These studies indicate progress in handling the complexities of benign versus malignant nodule classification, focusing on balancing sensitivity and false positive control.

For models that combine both nodule versus non-nodule and benign versus malignant classification, innovations in hybrid and transfer learning techniques have been instrumental. Lin et al. (2020) developed EDICNet, integrating RetinaNet with hierarchical convolutional networks, achieving an AUC of 0.89 for malignant prediction. Cai et al. (2023) enhanced classification performance through localized fine-tuning across multiple datasets, while Gugulothu and Balaji (2024) combined chaotic bird optimization with an improved fish-swarm algorithm to boost accuracy and sensitivity. Raza et al. (2023) demonstrated the effectiveness of Lung-EffNet, achieving 99.10% accuracy on the IQ-OTH/NCCD dataset, addressing class imbalance with data augmentation techniques. These innovations highlight the critical role of advanced optimization and hybrid learning in achieving high accuracy across multiple classification tasks.

Regarding Computational Complexity: Recent studies indicate that improvements in pulmonary nodule classification often come with increased computational demands. Chen et al. (2021) reported higher complexity for their DenseNet model despite improved accuracy. Naqi et al. (2020) and Dodia et al. (2022) both enhanced model sensitivity but at the cost of increased computational burden. Lei et al. (2020) similarly found their SAM and HESAM methods added significant complexity. In contrast, Suresh and Mohan (2022) achieved high accuracy with relatively low computational overhead, emphasizing efficiency-focused design. These findings suggest that balancing performance with computational efficiency is key to making AI models viable for clinical use.

Model Adoption and Clinical Implications: The adoption of AI-driven classification models in clinical workflows requires balancing model performance with computational efficiency. High-performing models like DenseNet, employed by Chen et al. (2021), improve performance but add computational complexity. Similarly, Naqi et al.'s (2020) FODPSO-based method successfully reduced false positives but at the cost of increased computational requirements. Conversely, Suresh and Mohan (2022) employed a DCNN that maintained high accuracy with lower computational costs, making it more feasible for clinical integration. These examples illustrate the ongoing challenge of achieving high accuracy while maintaining computational feasibility, which is essential for broader clinical adoption, particularly in resource-limited settings.

Future Directions and Clinical Potential: Future research should focus on the development of computationally efficient models suitable for deployment in real-time clinical settings, particularly those with limited resources. Lightweight models capable of functioning on mobile devices could dramatically improve accessibility to high-quality diagnostic tools, especially in underserved areas. Moreover, the integration of imaging data with other modalities, such as genomic and biomarker information, presents a promising direction for enhancing diagnostic precision and providing a more comprehensive understanding of the patient's condition. Ultimately, AI-driven classification models have made significant progress in distinguishing between benign and malignant nodules, enhancing early detection and reducing unnecessary interventions. To fully realize their clinical potential, continued focus on optimizing computational efficiency, accuracy, and data integration will be key to ensuring these tools benefit diverse healthcare environments.

Subtyping nodules enables more precise clinical decisions: we specifically discuss the subclassification of lung nodules—beyond the traditional benign/malignant dichotomy—to emphasize its clinical significance. Ground-glass nodules (GGNs), for example, are often early indicators of adenocarcinoma, whereas calcified nodules tend to be benign; recognizing these differences can directly influence follow-up intervals, biopsy decisions, and surgical planning. Recent studies demonstrate the feasibility of this finer-grained analysis: Naveen et al. (2023) report subtype-specific performance on LIDC-IDRI of 90.86% for solid, 93.68% for part-solid, and 97.06% for non-solid nodules; Guo et al. (2023) and Sivakumar et al. (2024) achieve over 95% accuracy on

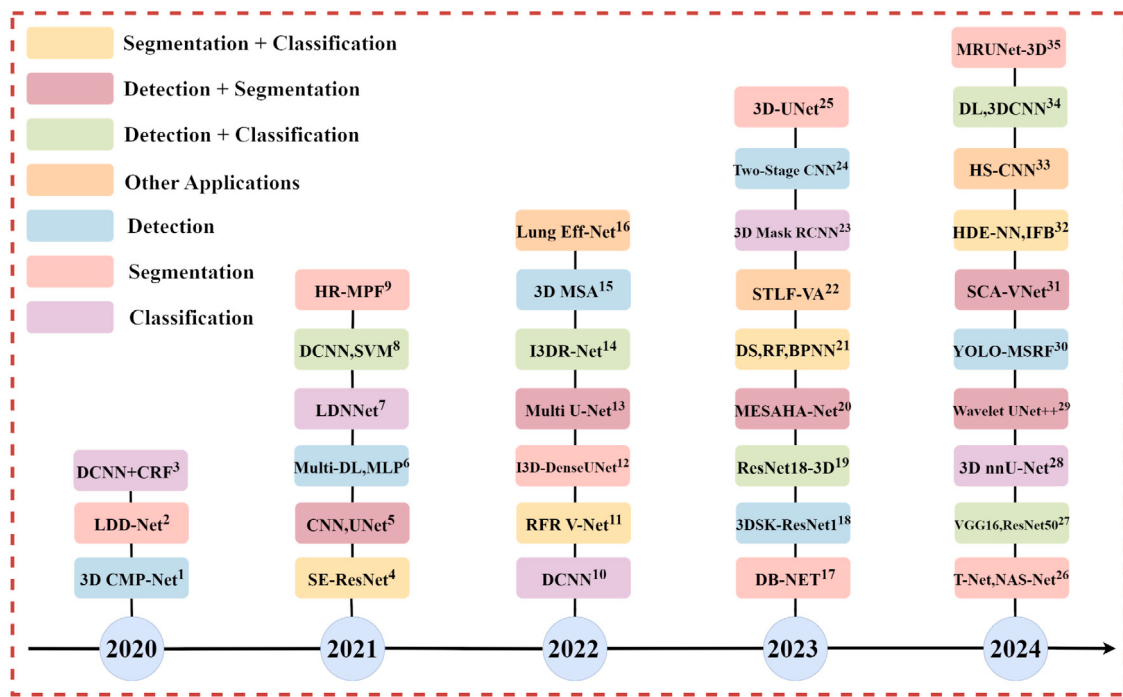


Fig. 11. Timeline of AI-driven advancements in lung cancer detection, segmentation, and classification (2020–2024). Colors represent application areas: Segmentation + Classification (yellow), Detection + Segmentation (pink), Detection + Classification (green), Other Applications (orange), Detection (blue), Segmentation (red), and Classification (purple). Each node represents a key model or method with performance metrics, highlighting major breakthroughs. Superscript numbers next to models indicate their corresponding references: 1–3 (Song et al., 2020; Chen et al., 2020; Savitha and Jidesh, 2020), 4–9 (Zhang et al., 2021; Osadebey et al., 2021; Fu et al., 2021; Chen et al., 2021; Muzammil et al., 2021; Zhu et al., 2021b), 10–16 (Suresh and Mohan, 2022; Dodia et al., 2022; Zhang et al., 2022b; Ni et al., 2022; Harsono et al., 2022; Zhang et al., 2022a; Raza et al., 2023), 17–25 (Bhattacharyya et al., 2023; Zhang and Zhang, 2023; Cai et al., 2023; Usman et al., 2023; Naveen et al., 2023; Wu et al., 2023a; Cai et al., 2023; Jain et al., 2023; Youssef et al., 2023), 26–35 (Thangavel and Palanichamy, 2024; Atiya et al., 2024; Wang et al., 2024; Agnes et al., 2024; Wu et al., 2024b; Liu et al., 2024; Gugulothu and Balaji, 2024; Lin et al., 2020, 2024a; Bbosa et al., 2024).

benign versus malignant classification, providing a strong foundation for multi-class extensions; and Zhang et al. (2021, 2022) incorporate segmentation and multi-task learning to fuse morphological and contextual features, further improving subtype discrimination. These advancements in multi-class classification and multi-task frameworks offer a more nuanced and clinically actionable approach to pulmonary CAD systems.

FDA clearance validates AI lung CAD for clinical use: we have added the following discussion of FDA-cleared AI systems to illustrate their clinical translation: Several AI systems for lung nodule detection and classification have obtained FDA clearance, demonstrating the readiness of deep learning-based CAD tools for clinical deployment. Optellum Lung Cancer Prediction (2021) leverages a deep learning-derived “lung cancer prediction score” trained on over 300,000 CT scans; a retrospective study in Radiology (2021) reported a 12%–20% increase in pulmonologist diagnostic accuracy and a significant reduction in unnecessary follow-ups. Arterys Lung AI (2020) provides automated nodule detection, classification, and volumetric tracking via cloud-PACS integration, reporting robust performance on multi-institutional datasets for both solid and subsolid nodules. Although CT-based systems dominate, Lunit INSIGHT CXR (2021) earned FDA clearance for chest X-ray-based detection of ten thoracic abnormalities—including nodules—achieving an AUC of 0.974 in a clinical validation of over 100,000 images. Finally, VUNO Med-LungCT AI, cleared under Korea’s 510(k) pathway and pending FDA approval, has demonstrated > 90% sensitivity in multicenter Korean CT cohorts and is now integrated into early lung-cancer screening workflows. These examples underscore the importance of explainability, regulatory compliance, and seamless integration into clinical systems when translating deep learning methods from research to routine practice.

Through an in-depth analysis of the aforementioned studies on lung cancer detection, segmentation, and classification, Fig. 11 summarizes and presents the significant advancements made in these areas

from 2020 to 2024. It comprehensively reflects the applications and performance improvements of deep learning models in pulmonary nodule analysis. The figure covers the evolution of single-task models (e.g., DCNN, 3D U-Net) and multi-task fusion models (e.g., ResNet18-3D, STLF-VA), clearly illustrating the trend of continuous optimization and integration of these technologies. With the introduction of advanced approaches such as YOLO-MSRF, I3DR-Net, and Wavelet U-Net++, AI-driven computer-aided diagnosis (CAD) systems have significantly enhanced detection sensitivity, segmentation precision, and classification accuracy. These systems demonstrate considerable potential, particularly in multi-task processing and complex network architectures. Notably, these models have achieved breakthroughs not only in improving early diagnosis and reducing misdiagnosis rates but also in providing robust support for real-world clinical applications. The developments outlined in Fig. 11 indicate that future trends will focus on multi-modal integration, automated feature extraction, and improving model generalization, thereby laying a solid technical foundation for early detection and accurate diagnosis of pulmonary nodules.

6. Challenges and future prospects

AI-driven advancements in lung cancer detection, segmentation, and classification have shown significant potential in improving diagnostic accuracy and efficiency. However, several challenges remain that hinder the full deployment and adoption of these technologies in clinical settings.

Data. A major challenge lies in the availability and quality of data. Although datasets like LIDC-IDRI and LUNA16 have been instrumental in advancing AI-based models for lung cancer analysis, these datasets are limited in scope and may not represent the full diversity of clinical cases. Furthermore, high-quality, annotated datasets are essential for training robust models, yet current datasets often suffer from annotation inconsistencies and a lack of standardization across institutions.

The quality of CT images, including issues such as noise, motion artifacts, and variations in acquisition protocols, further complicates model training. These data challenges limit the generalizability of AI models and their robustness in real-world applications.

Algorithms. Selecting the appropriate algorithm for different tasks, such as detection, segmentation, and classification, remains a complex issue. Deep learning algorithms like CNNs, U-Net, and their variants have demonstrated strong performance, but they also present challenges in terms of model interpretability and computational cost. Many models function as “black boxes”, making it difficult for clinicians to understand the decision-making process behind a model’s predictions, potentially limiting clinical adoption. Moreover, there is a need for algorithms that are not only accurate but also computationally efficient to enable real-time diagnosis in resource-constrained environments.

Tasks. Current lung cancer CAD systems predominantly focus on well-defined tasks such as nodule detection, segmentation, and binary classification (benign vs. malignant). However, these tasks may not fully capture the complexity of lung cancer diagnosis. More nuanced tasks, such as predicting tumor growth or treatment response, require further exploration. Additionally, while most models focus on 2D image data from CT scans, there is an increasing need to integrate 3D data, multi-modal inputs (such as PET-CT), and even temporal data (such as follow-up scans) to better characterize the progression of lung cancer. This broader scope of tasks will require more sophisticated models capable of handling diverse and complex data types.

Tools. Although AI models have demonstrated impressive capabilities, there is still a significant gap in providing accessible tools for non-expert users, such as radiologists and clinicians, who may lack extensive programming knowledge. The development of user-friendly platforms that integrate classical machine learning and deep learning algorithms, offering ready-to-use tools for model training, evaluation, and interpretation, is crucial. Such platforms should allow clinicians to apply advanced AI models without needing to write complex code, thus reducing the time and technical barriers to AI adoption in clinical practice.

Generalizability and Validation. One of the major hurdles in implementing AI-driven CAD systems in real-world clinical settings is ensuring that models generalize well across different institutions and populations. Models trained on a specific dataset may not perform as expected when applied to data from a different hospital or region due to variations in imaging protocols, equipment, and patient demographics. Rigorous external validation across diverse datasets is required to address this issue. Additionally, cross-platform compatibility should be emphasized, ensuring that AI models can be effectively deployed across a range of hardware configurations, from high-performance servers to mobile devices.

In summary, AI-driven lung cancer diagnosis faces multiple challenges related to data, algorithms, tasks, tools, and generalizability, requiring reliable solutions to fully harness the potential of these technologies. Future research directions should focus on the following areas:

1. **Building large, diverse datasets:** Expanding publicly available datasets with a broader range of imaging modalities (e.g., CT, PET, MRI) and clinical contexts (e.g., early-stage vs. late-stage lung cancer) to improve model robustness and generalizability.
2. **Data augmentation and synthetic data:** Leveraging deep learning-based techniques such as GANs, to augment existing datasets and generate synthetic data, addressing issues of data scarcity and overfitting during model training.
3. **Developing interpretable AI models:** Enhancing model transparency by integrating explainability methods, such as attention mechanisms or post-hoc interpretability tools, to help clinicians better understand AI predictions.

4. **Creating efficient algorithms for real-time applications:** Designing lightweight, high-performance models that can be deployed in real-time diagnostic scenarios, particularly in resource-constrained environments such as rural clinics or mobile devices.
5. **Expanding task scope:** Incorporating more complex tasks, such as longitudinal tumor tracking and multi-modal data integration, to provide a more comprehensive diagnostic tool for lung cancer management.
6. **Building user-friendly AI platforms:** Developing zero-code or low-code platforms that allow clinicians to easily apply AI models, assess model performance, and generate predictions without requiring programming expertise.
7. **Enhancing cross-institution generalizability:** Promoting external validation and cross-platform compatibility to ensure that AI models can generalize effectively across different clinical settings and patient populations.

These future directions will be essential in overcoming the current challenges in AI-driven lung cancer diagnosis, making these technologies more accessible and reliable for clinical applications.

7. Conclusion

Deep learning has revolutionized medical image analysis, particularly in the early detection of lung cancer, where it surpasses traditional statistical methods in handling complex data. Despite notable advances in pulmonary nodule detection, segmentation, and classification using CNNs, RNNs, and GANs, challenges such as data scarcity and the interpretability of models remain. The reliance on large, annotated datasets limits the widespread clinical application of these models, while their “black box” nature raises concerns about transparency in medical decision-making. Future research should focus on enhancing model interpretability through explainable AI (XAI) techniques and overcoming data limitations with innovative solutions like GAN-based augmentation. Furthermore, integrating multimodal data—such as genomic and clinical information—into CAD systems and exploring hybrid models that combine deep learning with traditional machine learning could significantly improve diagnostic accuracy and clinical utility. By addressing these challenges, deep learning holds immense potential to further transform early lung cancer detection and patient outcomes. This review aims to provide valuable insights to guide future research in this evolving field.

CRediT authorship contribution statement

Guohui Cai: Writing – original draft, Methodology, Investigation, Conceptualization. **Ying Cai:** Writing – original draft, Validation, Investigation. **Zeyu Zhang:** Writing – original draft. **Yuanzhouhan Cao:** Writing – review & editing, Methodology. **Lin Wu:** Methodology, Investigation. **Daji Ergu:** Supervision. **Zhibin Liao:** Methodology, Investigation. **Yang Zhao:** Supervision, Investigation.

Declaration of competing interest

All authors declare no conflicts of interest relevant to this study.

Acknowledgments

This research has been supported by the National Natural Science Foundation of China (Grant No. 72174172) and the Scientific and Technological Innovation Team for Qinghai-Tibetan Plateau Research at Southwest Minzu University (Grant No. 2024CXTD20). We sincerely appreciate their valuable support, which made this work possible.

Data availability

"I have shared the link to my code in the manuscript: <https://github.com/CaiGuoHui123/Awesome-Lung-Cancer-Detection>".

References

- Aerts, H.J., Velazquez, E.R., Leijenaar, R.T., Parmar, C., Grossmann, P., Carvalho, S., Bussink, J., Monshouwer, R., Haibe-Kains, B., Rietveld, D., et al., 2014. Decoding tumour phenotype by noninvasive imaging using a quantitative radiomics approach. *Nat. Commun.* 5 (1), 4006.
- Agnes, S.A., Anitha, J., Solomon, A.A., 2022. Two-stage lung nodule detection framework using enhanced unet and convolutional LSTM networks in CT images. *Comput. Biol. Med.* 149, 106059.
- Agnes, S.A., Solomon, A.A., Karthick, K., 2024. Wavelet U-net++ for accurate lung nodule segmentation in CT scans: Improving early detection and diagnosis of lung cancer. *Biomed. Signal Process. Control.* 87, 105509.
- Ahmadyar, Y., Kamali-Asl, A., Arabi, H., Samimi, R., Zaidi, H., 2024. Hierarchical approach for pulmonary-nodule identification from CT images using YOLO model and a 3D neural network classifier. *Radiol. Phys. Technol.* 17 (1), 124–134.
- Amini, F., Amjadifard, R., Mansouri, A., 2024. Fuzzy information granulation towards benign and malignant lung nodules classification. *Comput. Methods Programs Biomed.* Updat. 5, 100153.
- Armato, III, S.G., McLennan, G., Bidaut, L., McNitt-Gray, M.F., Meyer, C.R., Reeves, A.P., Zhao, B., Aberle, D.R., Henschke, C.I., Hoffman, E.A., et al., 2011. The lung image database consortium (LIDC) and image database resource initiative (IDRI): a completed reference database of lung nodules on CT scans. *Med. Phys.* 38 (2), 915–931.
- Asiya, S., Sugitha, N., 2024. Automatically segmenting and classifying the lung nodules from ct images. *Int. J. Intell. Syst. Appl. Eng.* 12 (1s), 271–281.
- Atiya, S.U., Ramesh, N., Reddy, B.N.K., 2024. Classification of non-small cell lung cancers using deep convolutional neural networks. *Multimedia Tools Appl.* 83 (5), 13261–13290.
- Balannolla, S., Nikhath, A.K., Yeruva, S., 2022. Detection and classification of lung carcinoma using CT scans. In: *Journal of Physics: Conference Series*, vol. 2286, IOP Publishing, 012011.
- Bawack, R.E., Fosso Wamba, S., Carillo, K.D.A., 2021. A framework for understanding artificial intelligence research: insights from practice. *J. Enterp. Inf. Manag.* 34 (2), 645–678.
- Bbosa, R., Gui, H., Luo, F., Liu, F., Efio-Akolly, K., Chen, Y.-P.P., 2024. MRUNet-3D: A multi-stride residual 3D unet for lung nodule segmentation. *Methods* 226, 89–101.
- Bhaskar, N., Ganashree, T.S., Patra, R.K., 2023. Pulmonary lung nodule detection and classification through image enhancement and deep learning. *Int. J. Biom.* 15 (3–4), 291–313.
- Bhatt, S.D., Soni, H.B., Pawar, T.D., Kher, H.R., 2022. Diagnosis of pulmonary nodules on CT images using YOLOv4. *Int. J. Online Biomed. Eng.* 18 (5).
- Bhattacharyya, D., Thirupathi Rao, N., Joshua, E.S.N., Hu, Y.-C., 2023. A bi-directional deep learning architecture for lung nodule semantic segmentation. *Vis. Comput.* 39 (11), 5245–5261.
- Bian, C., Xia, N., Yang, X., Wang, F., Wang, F., Wei, B., Dong, Q., 2024. MambaClinix: Hierarchical gated convolution and mamba-based U-net for enhanced 3D medical image segmentation. *arXiv preprint arXiv:2409.12533*.
- Blanc, D., Racine, V., Khalil, A., Deloche, M., Broyelle, J.-A., Hammouamri, I., Sinitambirivoutin, E., Fiammante, M., Verdier, E., Besson, T., et al., 2020. Artificial intelligence solution to classify pulmonary nodules on CT. *Diagn. Interv. Imaging* 101 (12), 803–810.
- Bray, F., Laversanne, M., Sung, H., Ferlay, J., Siegel, R.L., Soerjomataram, I., Jemal, A., 2024. Global cancer statistics 2022: GLOBOCAN estimates of incidence and mortality worldwide for 36 cancers in 185 countries. *CA: Cancer J. Clin.* 74 (3), 229–263.
- Budati, M., Karumuri, R., 2024. An intelligent lung nodule segmentation framework for early detection of lung cancer using an optimized deep neural system. *Multimedia Tools Appl.* 83 (12), 34153–34174.
- Cai, G., Cai, Y., Zhang, Z., Ergu, D., Cao, Y., Hu, B., Liao, Z., Zhao, Y., 2024a. MSDet: Receptive field enhanced multiscale detection for tiny pulmonary nodule. *arXiv preprint arXiv:2409.14028*.
- Cai, J., Guo, L., Zhu, L., Xia, L., Qian, L., Lure, Y.-M.F., Yin, X., 2023. Impact of localized fine tuning in the performance of segmentation and classification of lung nodules from computed tomography scans using deep learning. *Front. Oncol.* 13, 1140635.
- Cai, Y., Liu, Z., Zhang, Y., Yang, Z., 2024b. MDFN: A multi-level dynamic fusion network with self-calibrated edge enhancement for lung nodule segmentation. *Biomed. Signal Process. Control.* 87, 105507.
- Cai, L., Long, T., Dai, Y., Huang, Y., 2020. Mask R-CNN-based detection and segmentation for pulmonary nodule 3D visualization diagnosis. *IEEE Access* 8, 44400–44409.
- Cao, H., Liu, H., Song, E., Ma, G., Xu, X., Jin, R., Liu, T., Hung, C.-C., 2020. A two-stage convolutional neural networks for lung nodule detection. *IEEE J. Biomed. Heal. Inform.* 24 (7), 2006–2015.
- Chen, Y., Hou, X., Yang, Y., Ge, Q., Zhou, Y., Nie, S., 2023. A novel deep learning model based on multi-scale and multi-view for detection of pulmonary nodules. *J. Digit. Imaging* 36 (2), 688–699.
- Chen, Y., Wang, Y., Hu, F., Feng, L., Zhou, T., Zheng, C., 2021. LDNNET: towards robust classification of lung nodule and cancer using lung dense neural network. *IEEE Access* 9, 50301–50320.
- Chen, Y., Wang, Y., Hu, F., Wang, D., 2020. A lung dense deep convolution neural network for robust lung parenchyma segmentation. *IEEE Access* 8, 93527–93547.
- Chi, J., Zhao, J., Wang, S., Yu, X., Wu, C., 2024. LGDNet: local feature coupling global representations network for pulmonary nodules detection. *Med. Biol. Eng. Comput.* 1–14.
- Cortes, C., Vapnik, V., 1995. Support-vector networks. *Mach. Learn.* 20, 273–297.
- Cover, T., Hart, P., 1967. Nearest neighbor pattern classification. *IEEE Trans. Inform. Theory* 13 (1), 21–27.
- arXiv preprint arXiv:2405.21060.
- de Mesquita, V.A., Cortez, P.C., Ribeiro, A.B., de Albuquerque, V.H.C., 2022. A novel method for lung nodule detection in computed tomography scans based on boolean equations and vector of filters techniques. *Comput. Electr. Eng.* 100, 107911.
- de Pinho Pinheiro, C.A., Nedjah, N., de Macedo Mourelle, L., 2020. Detection and classification of pulmonary nodules using deep learning and swarm intelligence. *Multimedia Tools Appl.* 79 (21), 15437–15465.
- Dodia, S., Basava, A., Padukudu Anand, M., 2022. A novel receptive field-regularized V-net and nodule classification network for lung nodule detection. *Int. J. Imaging Syst. Technol.* 32 (1), 88–101.
- Drishti, Singh, J., 2024. Novel algorithm for pulmonary nodule classification using CNN on CT scans. *Int. J. Intell. Syst. Appl. Eng.* 12 (2), 144–152.
- Dutande, P., Baid, U., Talbar, S., 2021. LNCDs: A 2D-3D cascaded CNN approach for lung nodule classification, detection and segmentation. *Biomed. Signal Process. Control.* 67, 102527.
- El-Bana, S., Al-Kabbany, A., Sharkas, M., 2020. A two-stage framework for automated malignant pulmonary nodule detection in CT scans. *Diagnostics* 10 (3), 131.
- Farhangi, M.M., Sahiner, B., Petrick, N., Pezeshk, A., 2021. Automatic lung nodule detection in thoracic CT scans using dilated slice-wise convolutions. *Med. Phys.* 48 (7), 3741–3751.
- Fu, Y., Xue, P., Li, N., Zhao, P., Xu, Z., Ji, H., Zhang, Z., Cui, W., Dong, E., 2021. Fusion of 3D lung CT and serum biomarkers for diagnosis of multiple pathological types on pulmonary nodules. *Comput. Methods Programs Biomed.* 210, 106381.
- Gao, Z., Guo, Y., Wang, G., Chen, X., Cao, X., Zhang, C., An, S., Xu, F., 2024. Robust deep learning from incomplete annotation for accurate lung nodule detection. *Comput. Biol. Med.* 173, 108361.
- Gautam, N., Basu, A., Sarkar, R., 2024. Lung cancer detection from thoracic CT scans using an ensemble of deep learning models. *Neural Comput. Appl.* 36 (5), 2459–2477.
- Ge, J., Zhang, Z., Phan, M.H., Zhang, B., Liu, A., Zhao, Y., 2024. Esa: Annotation-efficient active learning for semantic segmentation. *arXiv preprint arXiv:2408.13491*.
- Gonidakis, P., Sónora Mengana, A., Jansen, B., Vandemeulebroucke, J., 2023. Hand-crafted features can boost performance and data-efficiency for deep detection of lung nodules from CT imaging. *IEEE Access* 11, 126221–126231.
- Goodfellow, I., Pouget-Abadie, J., Mirza, M., Xu, B., Warde-Farley, D., Ozair, S., Courville, A., Bengio, Y., 2014. Generative adversarial nets. *Adv. Neural Inf. Process. Syst.* 27.
- Gu, A., Dao, T., 2023. Mamba: Linear-time sequence modeling with selective state spaces. *arXiv preprint arXiv:2312.00752*.
- Gugulothu, V.K., Balaji, S., 2023. A novel deep learning approach for the detection and classification of lung nodules from ct images. *Multimedia Tools Appl.* 82 (30), 47611–47634.
- Gugulothu, V.K., Balaji, S., 2024. An early prediction and classification of lung nodule diagnosis on ct images based on hybrid deep learning techniques. *Multimedia Tools Appl.* 83 (1), 1041–1061.
- Guo, Z., Yang, J., Zhao, L., Yuan, J., Yu, H., 2023. 3D SAACNet with GBM for the classification of benign and malignant lung nodules. *Comput. Biol. Med.* 153, 106532.
- Gupta, H., Singh, H., Kumar, A., 2024. Texture and radiomics inspired data-driven cancerous lung nodules severity classification. *Biomed. Signal Process. Control.* 88, 105543.
- Halder, A., Chatterjee, S., Dey, D., Kole, S., Munshi, S., 2020. An adaptive morphology based segmentation technique for lung nodule detection in thoracic CT image. *Comput. Methods Programs Biomed.* 197, 105720.
- Halder, A., Dey, D., 2023. Atrous convolution aided integrated framework for lung nodule segmentation and classification. *Biomed. Signal Process. Control.* 82, 104527.
- Harsono, I.W., Liawatimena, S., Cenggoro, T.W., 2022. Lung nodule detection and classification from thorax CT-scan using RetinaNet with transfer learning. *J. King Saud University- Comput. Inf. Sci.* 34 (3), 567–577.
- He, K., Zhang, X., Ren, S., Sun, J., 2016. Deep residual learning for image recognition. In: *Proceedings of the IEEE Conference on Computer Vision and Pattern Recognition*. pp. 770–778.

- Hendrix, W., Hendrix, N., Scholten, E.T., Mourits, M., Trap-de Jong, J., Schalekamp, S., Korst, M., van Leuken, M., van Ginneken, B., Prokop, M., et al., 2023. Deep learning for the detection of benign and malignant pulmonary nodules in non-screening chest CT scans. *Commun. Med.* 3 (1), 156.
- Henschke, C.I., McCauley, D.I., Yankelevitz, D.F., Naidich, D.P., McGuinness, G., Miettinen, O.S., Libby, D., Pasmantier, M., Koizumi, J., Altorki, N., et al., 2001. Early lung cancer action project: a summary of the findings on baseline screening. *Oncol.* 6 (2), 147–152.
- Hiwase, A.D., Ovenden, C.D., Kaukas, L.M., Finnis, M., Zhang, Z., O'Connor, S., Foo, N., Reddi, B., Wells, A.J., Ellis, D.Y., 2024. Can rotational thromboelastometry rapidly identify theragnostic targets in isolated traumatic brain injury? *Emerg. Med. Australas.*
- Hochreiter, S., Schmidhuber, J., 1997. Long short-term memory. *Neural Comput.* 9 (8), 1735–1780.
- Huang, G.-B., Zhu, Q.-Y., Siew, C.-K., 2006. Extreme learning machine: theory and applications. *Neurocomputing* 70 (1–3), 489–501.
- Hung, S.-C., Wang, Y.-T., Tseng, M.-H., 2023. An interpretable three-dimensional artificial intelligence model for computer-aided diagnosis of lung nodules in computed tomography images. *Cancers* 15 (18), 4655.
- Jain, S., Choudhari, P., Gour, M., 2023. Pulmonary lung nodule detection from computed tomography images using two-stage convolutional neural network. *Comput. J.* 66 (4), 785–795.
- Ji, Y., Saratchandran, H., Gordon, C., Zhang, Z., Lucey, S., 2024. Sine activated low-rank matrices for parameter efficient learning. *arXiv preprint arXiv:2403.19243*.
- Jian, M., Jin, H., Zhang, L., Wei, B., Yu, H., 2024. DBPNNet: dual-branch networks using 3DCNN toward pulmonary nodule detection. *Med. Biol. Eng. Comput.* 62 (2), 563–573.
- Jin, H., Yu, C., Gong, Z., Zheng, R., Zhao, Y., Fu, Q., 2023. Machine learning techniques for pulmonary nodule computer-aided diagnosis using CT images: A systematic review. *Biomed. Signal Process. Control.* 79, 104104.
- Kadhim, O.R., Motlak, H.J., Abdalla, K.K., 2022. Computer-aided diagnostic system kinds and pulmonary nodule detection efficacy. *Int. J. Electr. Comput. Engineering (IJECE)* 12 (5), 4734–4745.
- Kadia, D.D., Alom, M.Z., Burada, R., Nguyen, T.V., Asari, V.K., 2021. R 2 u3D: Recurrent residual 3D U-net for lung segmentation. *IEEE Access* 9, 88835–88843.
- Kalkseetharaman, P., George, S.T., 2024. A bird's eye view approach on the usage of deep learning methods in lung cancer detection and future directions using X-Ray and CT images. *Arch. Comput. Methods Eng.* 1–21.
- Karrar, A., Mabrouk, M.S., Abdel Wahed, M., Sayed, A.Y., 2023. Auto diagnostic system for detecting solitary and juxtapleural pulmonary nodules in computed tomography images using machine learning. *Neural Comput. Appl.* 35 (2), 1645–1659.
- Kaulgud, R.V., Patil, A., 2023. Analysis based on machine and deep learning techniques for the accurate detection of lung nodules from CT images. *Biomed. Signal Process. Control.* 85, 105055.
- Khanna, A., Londhe, N.D., Gupta, S., Semwal, A., 2020. A deep residual U-net convolutional neural network for automated lung segmentation in computed tomography images. *Biocybern. Biomed. Eng.* 40 (3), 1314–1327.
- Krizhevsky, A., Sutskever, I., Hinton, G.E., 2012. Imagenet classification with deep convolutional neural networks. *Adv. Neural Inf. Process. Syst.* 25.
- LeCun, Y., Bottou, L., Bengio, Y., Haffner, P., 1998. Gradient-based learning applied to document recognition. *Proc. IEEE* 86 (11), 2278–2324.
- Lei, Y., Tian, Y., Shan, H., Zhang, J., Wang, G., Kalra, M.K., 2020. Shape and margin-aware lung nodule classification in low-dose CT images via soft activation mapping. *Med. Image Anal.* 60, 101628.
- Lin, C.-Y., Guo, S.-M., Lien, J.-J., Lin, W.-T., Liu, Y.-S., Lai, C.-H., Hsu, I.-L., Chang, C.-C., Tseng, Y.-L., 2024a. Combined model integrating deep learning, radiomics, and clinical data to classify lung nodules at chest CT. *La Radiol. Medica* 129 (1), 56–69.
- Lin, C.-Y., Guo, S.-M., Lien, J.-J., Tsai, T.-Y., Liu, Y.-S., Lai, C.-H., Hsu, I.-L., Chang, C.-C., Tseng, Y.-L., 2024b. Development of a modified 3D region proposal network for lung nodule detection in computed tomography scans: a secondary analysis of lung nodule datasets. *Cancer Imaging* 24 (1), 40.
- Lin, Y., Wei, L., Han, S.X., Aberle, D.R., Hsu, W., 2020. EDICNet: An end-to-end detection and interpretable malignancy classification network for pulmonary nodules in computed tomography. In: *Medical Imaging 2020: Computer-Aided Diagnosis*, vol. 11314, SPIE, pp. 344–355.
- Liu, J., Li, Y., Li, W., Li, Z., Lan, Y., 2024. Multiscale lung nodule segmentation based on 3D coordinate attention and edge enhancement. *Electron. Res. Arch.* 32 (5), 3016–3037.
- Liu, S., Setio, A.A.A., Ghesu, F.C., Gibson, E., Grbic, S., Georgescu, B., Comaniciu, D., 2020. No surprises: Training robust lung nodule detection for low-dose CT scans by augmenting with adversarial attacks. *IEEE Trans. Med. Imaging* 40 (1), 335–345.
- Luo, Y., Cao, M., Chang, X., 2024. Pulmonary nodule segmentation network based on res select kernel contextual U-net. *J. Eng. Sci. Med. Diagn. Ther.* 7 (4), 041004.
- Ma, L., Li, G., Feng, X., Fan, Q., Liu, L., 2024a. TiCNet: Transformer in convolutional neural network for pulmonary nodule detection on CT images. *J. Imaging Inform. Med.* 37 (1), 196–208.
- Ma, X., Song, H., Jia, X., Wang, Z., 2024b. An improved V-Net lung nodule segmentation model based on pixel threshold separation and attention mechanism. *Sci. Rep.* 14 (1), 4743.
- Majidpourkhoei, R., Alilou, M., Majidzadeh, K., Babazadehsangar, A., 2021. A novel deep learning framework for lung nodule detection in 3d ct images. *Multimedia Tools Appl.* 80 (20), 30539–30555.
- Mao, Q., Zhao, S., Tong, D., Su, S., Li, Z., Cheng, X., 2021. Hessian-mrlod: Hessian information and multi-scale reverse LoG filter for pulmonary nodule detection. *Comput. Biol. Med.* 131, 104272.
- Masud, M., Muhammad, G., Hossain, M.S., Alhumyani, H., Alshamrani, S.S., Cheikhrouhou, O., Ibrahim, S., 2020. Light deep model for pulmonary nodule detection from CT scan images for mobile devices. *Wirel. Commun. Mob. Comput.* 2020 (1), 8893494.
- Mei, J., Cheng, M.-X., Xu, G., Wan, L.-R., Zhang, H., 2021. Sanet: A slice-aware network for pulmonary nodule detection. *IEEE Trans. Pattern Anal. Mach. Intell.* 44 (8), 4374–4387.
- Muzammil, M., Ali, I., Haq, I.U., Amir, M., Abdullah, S., 2021. Pulmonary nodule classification using feature and ensemble learning-based fusion techniques. *IEEE Access* 9, 113415–113427.
- Nair, S.S., Devi, D.V.M., Bhasi, D.S., 2022. Prediction and classification of CT images for early detection of lung cancer using various segmentation models. *Int. J. Electrical Electronics Res.* 10 (4), 1027–1035.
- Naqi, S.M., Sharif, M., Jaffar, A., 2020. Lung nodule detection and classification based on geometric fit in parametric form and deep learning. *Neural Comput. Appl.* 32 (9), 4629–4647.
- Naveen, H., Naveena, C., VN, M.A., 2023. An approach for classification of lung nodules. *Tumor Discov.* 2 (1), 317–317.
- Nguyen, T.-C., Nguyen, T.-P., Cao, T., Dao, T.T.P., Ho, T.-N., Nguyen, T.V., Tran, M.-T., 2023. MANet: Multi-branch attention auxiliary learning for lung nodule detection and segmentation. *Comput. Methods Programs Biomed.* 241, 107748.
- Ni, Y., Xie, Z., Zheng, D., Yang, Y., Wang, W., 2022. Two-stage multitask U-net construction for pulmonary nodule segmentation and malignancy risk prediction. *Quant. Imaging Med. Surg.* 12 (1), 292.
- Osadebey, M., Andersen, H.K., Waaler, D., Fossaa, K., Martinsen, A.C., Pedersen, M., 2021. Three-stage segmentation of lung region from CT images using deep neural networks. *BMC Med. Imaging* 21, 1–19.
- Qiu, J., Li, B., Liao, R., Mo, H., Tian, L., 2023. A dual-task region-boundary aware neural network for accurate pulmonary nodule segmentation. *J. Vis. Commun. Image Represent.* 96, 103909.
- Rahouma, K.H., Mabrouk, S.M., Aouf, M., 2024. Automated 3D convolutional neural network architecture design using genetic algorithm for pulmonary nodule classification. *Bull. Electr. Eng. Inform.* 13 (3), 2009–2018.
- Rashid, U., Jaffar, A., Rashid, M., Alshuhri, M.S., Akram, S., 2024. Nodule detection using local binary pattern features to enhance diagnostic decisions. *Comput. Mater. Contin.* 78 (3).
- Raza, R., Zulfiqar, F., Khan, M.O., Arif, M., Alvi, A., Iftikhar, M.A., Alam, T., 2023. Lung-EffNet: Lung cancer classification using EfficientNet from CT-scan images. *Eng. Appl. Artif. Intell.* 126, 106902.
- Rumelhart, D.E., Hinton, G.E., Williams, R.J., 1986. Learning representations by back-propagating errors. *Nature* 323 (6088), 533–536.
- Safta, W., Shaffie, A., 2024. Advancing pulmonary nodule diagnosis by integrating engineered and deep features extracted from CT scans. *Algorithms* 17 (4), 161.
- Savitha, G., Jidesh, P., 2020. A holistic deep learning approach for identification and classification of sub-solid lung nodules in computed tomographic scans. *Comput. Electr. Eng.* 84, 106626.
- Sengodan, P., Srinivasan, K., Pichamuthu, R., Matheswaran, S., 2023. Early detection and classification of malignant lung nodules from CT images: An optimal ensemble learning. *Expert Syst. Appl.* 229, 120361.
- Setio, A.A.A., Traverso, A., De Bel, T., Berens, M.S., Van Den Bogaard, C., Cerello, P., Chen, H., Dou, Q., Fantacci, M.E., Geurts, B., et al., 2017. Validation, comparison, and combination of algorithms for automatic detection of pulmonary nodules in computed tomography images: the LUNA16 challenge. *Med. Image Anal.* 42, 1–13.
- Shi, L., Ma, H., Zhang, J., 2021. Automatic detection of pulmonary nodules in CT images based on 3D res-i network. *Vis. Comput.* 37, 1343–1356.
- Siddiqui, E.A., Chaurasia, V., Shandilya, M., 2023. Detection and classification of lung cancer computed tomography images using a novel improved deep belief network with gabor filters. *Chemometr. Intell. Lab. Syst.* 235, 104763.
- Sivakumar, M., Chinnasamy, S., Thanabal, M., 2024. An efficient combined intelligent system for segmentation and classification of lung cancer computed tomography images. *PeerJ Comput. Sci.* 10, e1802.
- Song, T., Chen, J., Luo, X., Huang, Y., Liu, X., Huang, N., Chen, Y., Ye, Z., Sheng, H., Zhang, S., et al., 2020. CPM-net: A 3D center-points matching network for pulmonary nodule detection in CT scans. In: *International Conference on Medical Image Computing and Computer-Assisted Intervention*. Springer, pp. 550–559.
- Suji, R.J., Godfrey, W.W., Dhar, J., 2024. Exploring pretrained encoders for lung nodule segmentation task using LIDC-IDRI dataset. *Multimedia Tools Appl.* 83 (4), 9685–9708.
- Suresh, S., Mohan, S., 2022. NROI based feature learning for automated tumor stage classification of pulmonary lung nodules using deep convolutional neural networks. *J. King Saud University- Comput. Inf. Sci.* 34 (5), 1706–1717.
- Suzuki, K., Otsuka, Y., Nomura, Y., Kumamaru, K.K., Kuwatsuru, R., Aoki, S., 2022. Development and validation of a modified three-dimensional U-net deep-learning model for automated detection of lung nodules on chest ct images from the lung image database consortium and Japanese datasets. *Academic Radiol.* 29, S11–S17.

- Sweetline, B.C., Vijayakumaran, C., Samydurai, A., 2024. Overcoming the challenge of accurate segmentation of lung nodules: A multi-crop CNN approach. *J. Imaging Inform. Med.* 1–20.
- Tan, S., Zhang, Z., Cai, Y., Ergu, D., Wu, L., Hu, B., Yu, P., Zhao, Y., 2024. Segstitch: Multidimensional transformer for robust and efficient medical imaging segmentation. arXiv preprint [arXiv:2408.00496](https://arxiv.org/abs/2408.00496).
- Tang, T.-W., Lin, W.-Y., Liang, J.-D., Li, K.-M., 2023a. Artificial intelligence aided diagnosis of pulmonary nodules segmentation and feature extraction. *Clin. Radiol.* 78 (6), 437–443.
- Tang, T., Zhang, R., Lin, K., Li, F., Xia, X., 2023b. SM-RNet: A scale-aware-based multi-attention guided reverse network for pulmonary nodules segmentation. *IEEE Trans. Instrum. Meas.*
- Thangavel, C., Palanichamy, J., 2024. Effective deep learning approach for segmentation of pulmonary cancer in thoracic CT image. *Biomed. Signal Process. Control.* 89, 105804.
- Tyagi, S., Talbar, S.N., 2022. CSE-gan: A 3D conditional generative adversarial network with concurrent squeeze-and-excitation blocks for lung nodule segmentation. *Comput. Biol. Med.* 147, 105781.
- Usman, M., Rehman, A., Shahid, A., Latif, S., Byon, S.S., Kim, S.H., Khan, T.M., Shin, Y.G., 2023. MESAHA-net: Multi-encoders based self-adaptive hard attention network with maximum intensity projections for lung nodule segmentation in CT scan. arXiv preprint [arXiv:2304.01576](https://arxiv.org/abs/2304.01576).
- Usman, M., Rehman, A., Shahid, A., Latif, S., Shin, Y.-G., 2024. MEDS-net: Multi-encoder based self-distilled network with bidirectional maximum intensity projections fusion for lung nodule detection. *Eng. Appl. Artif. Intell.* 129, 107597.
- Van Ginneken, B., Armato, III, S.G., de Hoop, B., van Amelsvoort-van de Vorst, S., Duindam, T., Niemeijer, M., Murphy, K., Schilham, A., Retico, A., Fantacci, M.E., et al., 2010. Comparing and combining algorithms for computer-aided detection of pulmonary nodules in computed tomography scans: the ANODE09 study. *Med. Image Anal.* 14 (6), 707–722.
- Vaswani, A., 2017. Attention is all you need. *Adv. Neural Inf. Process. Syst.*
- Veronica, B.K., 2020. An effective neural network model for lung nodule detection in CT images with optimal fuzzy model. *Multimedia Tools Appl.* 79 (19), 14291–14311.
- Wang, C., Liu, Y., Wang, F., Zhang, C., Wang, Y., Yuan, M., Yang, G., 2024. Towards reliable and explainable AI model for pulmonary nodule diagnosis. *Biomed. Signal Process. Control.* 88, 105646.
- Wang, B., Si, S., Cui, E., Zhao, H., Yang, D., Dou, S., Zhu, J., 2020. A fast and efficient CAD system for improving the performance of malignancy level classification on lung nodules. *IEEE Access* 8, 40151–40170.
- Wang, B., Si, S., Zhao, H., Zhu, H., Dou, S., 2021. False positive reduction in pulmonary nodule classification using 3D texture and edge feature in CT images. *Technol. Health Care* 29 (6), 1071–1088.
- Wu, R., Liang, C., Li, Y., Shi, X., Zhang, J., Huang, H., 2023a. Self-supervised transfer learning framework driven by visual attention for benign–malignant lung nodule classification on chest CT. *Expert Syst. Appl.* 215, 119339.
- Wu, B., Xie, Y., Zhang, Z., Ge, J., Yaxley, K., Bahadir, S., Wu, Q., Liu, Y., To, M.-S., 2023b. BHSD: A 3D multi-class brain hemorrhage segmentation dataset. In: *International Workshop on Machine Learning in Medical Imaging*. Springer, pp. 147–156.
- Wu, B., Xie, Y., Zhang, Z., Phan, M.H., Chen, Q., Chen, L., Wu, Q., 2024a. Xlip: Cross-modal attention masked modelling for medical language-image pre-training. arXiv preprint [arXiv:2407.19546](https://arxiv.org/abs/2407.19546).
- Wu, X., Zhang, H., Sun, J., Wang, S., Zhang, Y., 2024b. YOLO-msrf for lung nodule detection. *Biomed. Signal Process. Control.* 94, 106318.
- Yang, H., Wang, Q., Zhang, Y., An, Z., Chen, L., Zhang, X., Zhou, S.K., 2023. Lung nodule segmentation and uncertain region prediction with an uncertainty-aware attention mechanism. *IEEE Trans. Med. Imaging.*
- Youssef, B., Alksas, A., Shalaby, A., Mahmoud, A., Van Bogaert, E., Alghamdi, N.S., Neubacher, A., Contractor, S., Ghazal, M., ElMaghraby, A., et al., 2023. Integrated deep learning and stochastic models for accurate segmentation of lung nodules from computed tomography images: a novel framework. *IEEE Access*.
- Yuan, H., Fan, Z., Wu, Y., Cheng, J., 2021. An efficient multi-path 3D convolutional neural network for false-positive reduction of pulmonary nodule detection. *Int. J. Comput. Assist. Radiol. Surg.* 16 (12), 2269–2277.
- Zhai, P., Tao, Y., Chen, H., Cai, T., Li, J., 2020. Multi-task learning for lung nodule classification on chest CT. *IEEE Access* 8, 180317–180327.
- Zhan, K., Wang, Y., Zhuo, Y., Zhan, Y., Yan, Q., Shan, F., Zhou, L., Chen, X., Liu, L., 2023. An uncertainty-aware self-training framework with consistency regularization for the multilabel classification of common computed tomography signs in lung nodules. *Quant. Imaging Med. Surg.* 13 (9), 5536.
- Zhang, Z., Ahmed, K.A., Hasan, M.R., Gedeon, T., Hossain, M.Z., 2024a. A deep learning approach to diabetes diagnosis. In: *Asian Conference on Intelligent Information and Database Systems*. Springer, pp. 87–99.
- Zhang, Z., Liu, A., Chen, Q., Chen, F., Reid, I., Hartley, R., Zhuang, B., Tang, H., 2024b. InfiniMotion: Mamba boosts memory in transformer for arbitrary long motion generation. arXiv preprint [arXiv:2407.10061](https://arxiv.org/abs/2407.10061).
- Zhang, Z., Liu, A., Reid, I., Hartley, R., Zhuang, B., Tang, H., 2024c. Motion mamba: Efficient and long sequence motion generation with hierarchical and bidirectional selective ssm. arXiv preprint [arXiv:2403.07487](https://arxiv.org/abs/2403.07487).
- Zhang, Y., Meng, L., 2022. Study on identification method of pulmonary nodules: Improved random walk pulmonary parenchyma segmentation and fusion multi-feature VGG16 nodule classification. *Front. Oncol.* 12, 822827.
- Zhang, H., Peng, Y., Guo, Y., 2022a. Pulmonary nodules detection based on multi-scale attention networks. *Sci. Rep.* 12 (1), 1466.
- Zhang, X., Pu, L., Wan, L., Wang, X., Zhou, Y., 2024d. DS-MSFF-net: Dual-path self-attention multi-scale feature fusion network for CT image segmentation. *Appl. Intell.* 54 (6), 4490–4506.
- Zhang, Z., Qi, X., Chen, M., Li, G., Pham, R., Qassim, A., Berry, E., Liao, Z., Siggs, O., McLaughlin, R., et al., 2024e. Jointvit: Modeling oxygen saturation levels with joint supervision on long-tailed octa. In: *Annual Conference on Medical Image Understanding and Analysis*. Springer, pp. 158–172.
- Zhang, Z., Qi, X., Zhang, B., Wu, B., Le, H., Jeong, B., Liao, Z., Liu, Y., Verjans, J., To, M.-S., et al., 2024f. Segreg: Segmenting oars by registering mr images and ct annotations. In: *2024 IEEE International Symposium on Biomedical Imaging*. ISBI, IEEE, pp. 1–5.
- Zhang, T., Wang, Y., Sun, Y., Yuan, M., Zhong, Y., Li, H., Yu, T., Wang, J., 2021. High-resolution CT image analysis based on 3D convolutional neural network can enhance the classification performance of radiologists in classifying pulmonary non-solid nodules. *Eur. J. Radiol.* 141, 109810.
- Zhang, G., Yang, Z., Jiang, S., 2022b. Automatic lung tumor segmentation from CT images using improved 3D densely connected UNet. *Med. Biol. Eng. Comput.* 60 (11), 3311–3323.
- Zhang, Z., Yi, N., Tan, S., Cai, Y., Yang, Y., Xu, L., Li, Q., Yi, Z., Ergu, D., Zhao, Y., 2024g. MedDet: Generative adversarial distillation for efficient cervical disc herniation detection. arXiv preprint [arXiv:2409.00204](https://arxiv.org/abs/2409.00204).
- Zhang, M., Yu, Y., Jin, S., Gu, L., Ling, T., Tao, X., 2024h. VM-UNET-V2: rethinking vision mamba unet for medical image segmentation. In: *International Symposium on Bioinformatics Research and Applications*. Springer, pp. 335–346.
- Zhang, H., Zhang, H., 2023. LungSeek: 3D selective kernel residual network for pulmonary nodule diagnosis. *Vis. Comput.* 39 (2), 679–692.
- Zhang, Z., Zhang, B., Hiwase, A., Barras, C., Chen, F., Wu, B., Wells, A.J., Ellis, D.Y., Reddi, B., Burgan, A.W., To, M.-S., Reid, I., Hartley, R., 2023. Thin-thick adapter: Segmenting thin scans using thick annotations. OpenReview.
- Zhang, X., Zhang, B., Liu, X., Dong, J., Zhao, S., Li, S., 2022c. Accurate classification of nodules and non-nodules from computed tomography images based on radiomics and machine learning algorithms. *Int. J. Imaging Syst. Technol.* 32 (3), 956–968.
- Zhang, J., Zou, W., Hu, N., Zhang, B., Wang, J., 2024i. S-net: an S-shaped network for nodule detection in 3D CT images. *Phys. Med. Biol.* 69 (7), 075013.
- Zhao, Y., Liao, Z., Liu, Y., Nijhuis, K.O., Barvelink, B., Prijs, J., Colaris, J., Wijffels, M., Reijman, M., Zhang, Z., et al., 2024. A landmark-based approach for instability prediction in distal radius fractures. In: *2024 IEEE International Symposium on Biomedical Imaging*. ISBI, IEEE, pp. 1–5.
- Zhao, D., Liu, Y., Yin, H., Wang, Z., 2023. An attentive and adaptive 3D CNN for automatic pulmonary nodule detection in CT image. *Expert Syst. Appl.* 211, 118672.
- Zhao, Y., Wang, Z., Liu, X., Chen, Q., Li, C., Zhao, H., Wang, Z., 2022. Pulmonary nodule detection based on multiscale feature fusion. *Comput. Math. Methods Med.* 2022 (1), 8903037.
- Zheng, S., Cornelissen, L.J., Cui, X., Jing, X., Veldhuis, R.N., Oudkerk, M., van Ooijen, P.M., 2021. Deep convolutional neural networks for multiplanar lung nodule detection: Improvement in small nodule identification. *Med. Phys.* 48 (2), 733–744.
- Zhu, H., Han, G., Peng, Y., Zhang, W., Lin, C., Zhao, H., 2021a. Functional-realistic CT image super-resolution for early-stage pulmonary nodule detection. *Future Gener. Comput. Syst.* 115, 475–485.
- Zhu, W., Liu, C., Fan, W., Xie, X., 2018. Deeplung: Deep 3d dual path nets for automated pulmonary nodule detection and classification. In: *2018 IEEE Winter Conference on Applications of Computer Vision*. WACV, IEEE, pp. 673–681.
- Zhu, L., Zhu, H., Yang, S., Wang, P., Yu, Y., 2021b. HR-MPF: high-resolution representation network with multi-scale progressive fusion for pulmonary nodule segmentation and classification. *EURASIP J. Image Video Process.* 2021, 1–26.